White matter abnormalities and structural hippocampal disconnections in Alzheimer's disease and amnestic mild cognitive impairment

Jared Rowley
Integrated Program of Neuroscience
McGill University, Montreal

Submitted February 2013

A thesis submitted to McGill University in partial fulfillment of the requirements of
the degree of Master of Science
© Jared Rowley 2013

Table of Contents

Abstract/Résumé

English

Objective: The purpose of this project was to evaluate white matter degeneration and its impact on hippocampal structural connectivity in patients with amnestic mild cognitive impairment, non-amnestic mild cognitive impairment and Alzheimer's disease.

Methods: We estimated white matter fractional anisotropy, mean diffusivity and hippocampal structural connectivity in two independent cohorts. The ADNI cohort included 108 subjects [25 cognitively normal, 21 amnestic mild cognitive impairment, 47 non-amnestic mild cognitive impairment and 15 Alzheimer's disease]. A second cohort included 34 subjects [15 cognitively normal and 19 amnestic mild cognitive impairment] recruited in Montreal. All subjects underwent clinical and neuropsychological assessment in addition to diffusion and T1 MRI. Individual fractional anisotropy and mean diffusivity maps were generated using FSL-DTIfit. In addition, hippocampal structural connectivity maps expressing the probability of connectivity between the hippocampus and cortex were generated using a pipeline based on FSL-probtrackX. Voxel-based group comparison statistics of fractional anisotropy, mean diffusivity and hippocampal structural connectivity were estimated using Tract-Based Spatial Statistics. The proportion of abnormal to total white matter volume was estimated using the total volume of the white matter skeleton.

Results: We found that in both cohorts, when compared to cognitively normal, amnestic mild cognitive impairment patients had 27-29% white matter volume showing higher mean diffusivity but no significant fractional anisotropy abnormalities. No fractional anisotropy or mean diffusivity differences were observed between non-amnestic between mild cognitive impairment patients and cognitively normal subjects. Alzheimer's disease patients had 66.3% of normalized

white matter volume with increased mean diffusivity and 54.3% of the white matter had reduced fractional anisotropy. Reduced structural connectivity was found in the hippocampal connections to temporal, inferior parietal, posterior cingulate and frontal regions only in the Alzheimer's group.

Conclusions: The severity of white matter degeneration appears to be higher in advanced clinical stages, supporting the construct that these abnormalities are part of the pathophysiological processes of Alzheimer's disease.

Français

Anormalités dans la matière blanche et déconnections structurelles de l'hippocampe dans la Maladie d'Alzheimer et le Trouble Cognitif Léger avec amnésie

Objectif: Ce projet a pour but d'évaluer la dégénérescence de la matière blanche et son impact sur la connectivité structurelle de l'hippocampe chez des patients avec un trouble cognitif léger avec ou sans amnésie ou la Maladie d'Alzheimer.

Méthodes: Nous avons estimé l'anisotropie fractionnelle et la diffusivité moyenne de la matière blanche ainsi que la connectivité structurelle de l'hippocampe dans deux cohortes indépendantes. La cohorte ADNI incluait 108 sujets [25 cognitivement normaux, 21 avec trouble cognitif léger avec amnésie, 47 avec trouble cognitif léger sans amnésie et 15 Maladie d'Alzheimer]. Une deuxième cohorte incluait 34 sujets [15 cognitivement normaux et 19 avec trouble cognitif léger avec amnésie] recrutés à Montréal. Tous les sujets ont passé une évaluation clinique et neuropsychologique, en plus d'acquisitions IRM de diffusion et T1. Les images individuelles d'anisotropie fractionnelle et de diffusivité moyenne ont été générées avec *FSL-DTIfit*. Celles de connectivité structurelle de l'hippocampe, qui expriment la probabilité d'une connexion entre l'hippocampe et le cortex, ont été générées en utilisant une fonction basée sur *FSL-probtractX*. Les comparaisons statistiques au niveau du voxel pour l'anisotropie fractionnelle, la diffusivité moyenne et la connectivité structurelle de l'hippocampe ont été estimées en utilisant l'outil *Tract-Based Spatial Statistics.* La proportion d'anormalités dans la matière blanche a été estimée en utilisant le volume total du patron de matière blanche.

Résultats: Dans les deux cohortes, on peut observer que les patients du groupe trouble cognitif léger avec amnésie ont 27-29% du volume de matière blanche avec une diffusivité moyenne plus élevée mais sans anormalité probante de l'anisotropie

fractionnelle. Aucune différence d'anisotropie fractionnelle ou de diffusivité moyenne n'est observée entre le groupe avec trouble cognitif léger sans amnésie et celui cognitivement normal. Nous avons trouvé chez les patients avec la Maladie d'Alzheimer 66.3% de la matière blanche normalisée avec une augmentation de la diffusivité moyenne, et dans 54.3% une réduction d'anisotropie fractionnelle. Une réduction de la connectivité structurelle a été détectée dans les connections hippocampales aux régions frontales, temporales, pariétales inférieures et cingulaires postérieures dans le groupe Maladie d'Alzheimer seulement.

Conclusions: La sévérité de la dégénérescence de la matière blanche apparaît être plus importante dans les stages cliniques avancées, ce qui supporte la théorie que ces anormalités font parties des processus pathophysiologiques de la Maladie d'Alzheimer.

Acknowledgments

Funding

Preface & Contribution of Authors

This thesis is a mandatory requirement for the degree of Master of Neuroscience at the integrated program of Neuroscience (IPN), McGill University. Credits for obtaining MSc were completed in May 2012 and the thesis seminar was successfully presented on June 21, 2012. Additionally, 11 credits were obtained after the successful completion of the following courses: Statistics for Neuroscience (PSYT 610), Computational Neuroscience (NUER 603) and Central Nervous System (NEUR 610).

The research presented in this thesis was entirely conducted at the Translational Neuroimaging Laboratory (TNL), McGill Centre for Studies in Aging at the Douglas Research Centre. All procedures and methods followed good laboratory practices, and current ethics and scientific integrity guidelines. It was my genuine choice to study the white matter abnormalities in aMCI and AD. I actively participated on the design, part of data acquisition, data analysis as well as drafted this thesis and its respective manuscript. The skills and expertise in neuroimaging to conduct the present research were entirely acquired at the TNL, and complemented in the FSL-Freesurfer diffusion weighted imaging course in San Francisco, California. Some steps of the analytical pipeline designed for this project was conducted under the guidance of imaging experts from the Montreal Neurological Institute, Aarhus and Harvard University. Other researchers in the lab are currently working with my pipelines.

I presented part of the results shown here as a poster at the Alzheimer's Association International conference in Paris France in July 2011. The manuscript presented within this thesis was submitted to PLoS ONE on February 16. Neither I nor any of my coauthors have any conflicting interest to disclose.

Experiments conception and designed: Jared Rowley and Pedro Rosa-Neto, Serge Gauthier, Amir Shmuel and Alain Dagher.

DTI data analysis: Jared Rowley

Neuropsychological testing for MCSA data: Dorothée Schoemaker and Viviane Sziklas

Analytical tools: Vladimir Fonov, Simon Eskildsen.

Statistical Analysis: Ona Wu and Pedro Rosa-Neto.

Analysis of ADNI neuropsychological data: Liyong Wu.

ADNI data organization and quality control: Sara Mohades and Monica Shin.

MCSA Clinical recruitment: Serge Gauthier

Drafting Manuscript: Jared Rowley

Manuscript supervision: Pedro Rosa-Neto Simon Eskildsen, Ona Wu, and Serge Gauthier.

Definitions and Abbreviations

ACC: anterior cingulate cortex.

AD: Alzheimer's disease: Neurodegenerative disease characterized by dementia associated to specific brain pathology such as neurofibrillary tangles and senile plaques.

Amyloid Plaques: accumulation of extracellular amyloid beta protein, a primary pathological feature of AD.

aMCI (Amnestic Mild Cognitive Impairment): syndrome characterized by objective memory impairment without dementia. aMCI is a prodromal manifestation of AD and other neurological conditions.

Biomarker: characteristic measured as an indicator of biological or pathogenic processes, or pharmacologic responses.

CA1, CA2, CA3 or CA4. Designation of four key hippocampal cellular fields commonly abbreviated as CA (Cornus Amonious, Ammon's horn in Latin)

CDR: Clinical Dementia Rating: Clinically used numeric scale of dementia rating based on 6 areas of cognitive performance where 0.5 is considered very mild [1].

CT: Computed tomography. 3d in vivo view of an object using x-rays

DTI: Diffusion Tensor Imaging. MRI sequence used to measure diffusion of water in vivo.

EC: Entorhinal Cortex.

FA: Fractional Anisotropy. Scalar number between 0 and 1 calculated from a DTI that describes the isotropy diffusion within a voxel.

GM: Gray Matter

Heterotypical cortices:

IPC: inferior parietal cortex.

MD: Mean Diffusivity. Scalar number calculated from mean of the 3 eigen values that describe the diffusion of water within a voxel.

MINC: Medical Image NetCDF. Image format (and tools) developed at the MNI for processing medical imaging files.

MMSE: Mini Mental State Examination. Short questionnaire used to measure cognitive impairment.

MNI Space: Coordinate system for anatomical landmarks based on the average of 152 t1 MRIs.

MRI: Magnetic Resonance Imaging

naMCI (Non-Amnestic Mild Cognitive Impairment): syndrome characterized by objective cognitive impairment other than memory without dementia.

Neurodegeneration: progressive loss of structure or function of neurons, including neuronal death.

NFT: Neurofibrillary tangles: Accumulation of hyperphosphorylated Tau proteins, a primary pathological feature of AD.

PCC: posterior cingulate cortex.

PFC: prefrontal cortex.

Preclinical AD: the long asymptomatic period between the first brain lesions and the first symptoms. It includes cognitively normal individuals who eventually develop AD dementia.

Prodromal AD: individuals with aMCI who eventually will develop dementia.

Prognostic markers describe molecular markers that predict disease-free survival, disease-specific survival, and overall survival.

ROIs: Region of Interest.

T1: Standard structural MRI.

Tractography: The process of identifying neuronal tracts within the brain.

WM: White Matter

Chapter 1: Introduction and Background

Introduction

Alzheimer's disease (AD) is a progressive neurological disease affecting nearly 11% of the Canadian population aged 65 and over [2]. It is taking an increasing toll on the health of aging Canadians, imposing a substantial burden on caregivers, costing the country billions of dollars in health care and lost wages. It is by far the most common form of dementia, representing 63% of all dementia cases [2]. The incidence of AD dramatically increases with age so that more than 1/3 of the population age 85 and older is affected [2]. Canadians spent $8 billion directly on healthcare care expenses related to dementia in 2008 while the disease cost an additional $7 billion in lost wages that year [2]. With the aging population it is estimated that Canadians will spend $93 billion per year on the treatment of patients with dementia by 2038 [2]. The physical, emotional, and financial toll associated with this disease make finding an effective treatment and an eventual cure of the utmost importance.

The progressive degenerative nature of the disease process in AD, and dementia more generally, poses tremendous obstacles to treatment and cure. The brains of demented individuals are riddled with structural damage forcing current efforts to focus on preventing rather than reversing the damage caused by the disease process. This reality makes research into detection of individuals at high risk of developing the disease particularly important. Although this area is fraught with challenges, some promising technologies have been developed, expanding the possibilities to identify individuals at high risk of developing dementia.

Mild cognitive impairment (MCI) is an intermediary stage between the preclinical and dementia stage of AD [3]. A patient with MCI has objective cognitive deficits which does not interfere notably with activities of daily life [3]. MCI patients progress to dementia at a rate of 16.5% per year [4]. As AD accounts for the majority of all forms of dementia [2], patients with MCI constitute an important subgroup to

study. Therefore, understanding of MCI neurobiology is critical to understanding AD.

Regarding neuropathology, MCI resembles the classic neuropathological features of early AD. The neuropathology of AD is defined by accumulation of beta-amyloid plaques, neurofibrillary tangles, and neuronal loss particularly in the hippocampus and the entorhinal cortex [5]. It is commonly believed that AD neuropathology progressively accumulates throughout the brain many years before the onset of symptoms (perhaps even decades) [5]. Evidence pointing towards this conclusion has been shown in a number of studies. Amyloidosis and limbic deposition of neurofibrillary tangles have been consistently demonstrated in MCI patients [6-9]. Regarding cell loss, Gomez-Isla et al. showed a 57% decline in total number of neurons in layer II of the entorhinal cortex, in MCI patients [7]. Perhaps even more interesting, a post mortem study of 134 specimens with clinical MCI showed that 54.4% of these subjects could be pathologically diagnosed as having AD [9]. In contrast with AD, the brains of MCI individuals display early stages of AD pathology (i.e. mild loss of neurons, and less accumulation of plaques and tangles). Pharmacological intervention in aMCI brings the hope of arresting or at least delaying the progression of AD [10]. As such, early detection of AD is an important step towards the prevention of dementia caused by AD.

Peterson and colleagues outlined a classification of MCI patients [11]. MCI is subdivided into amnestic mild cognitive impairment (aMCI) and non-amnestic mild cognitive impairment (naMCI), based on the predominance of memory impairment over other cognitive domains. The classification further dichotomizes into single and multiple domain. For example, the term 'aMCI single domain' applies if memory impairment constitutes the lone cognitive deficit in an individual. In contrast, the term 'aMCI multiple domain' defines an aMCI individual possessing additional cognitive impairments. In the present study, we will utilize Peterson's definitions of aMCI and naMCI. Additionally, individuals who are cognitive normal (CN) will designate participants without any cognitive deficits. The term CN better describes elderly populations rather than the terminology "normal" or "healthy elderly

individuals" as these CN individuals could develop cognitive complaints in the future.

aMCI is of significant interest for researchers because memory complaints are an early symptom of AD. It is hypothesized that aMCI individuals are more likely to convert to AD than naMCI; however, there isn't a scientific consensus yet. Some authors, such as Roundtree et al., [12] have found a higher rate of conversion to AD in aMCI individuals as opposed to naMCI.

Background

Relevance of White Matter

There is a growing consensus that white matter degeneration in aMCI and AD constitute a continuum. Chen and colleagues [13] proposed that white matter pathology, as measured *in-vivo in* dementia patients, may be a sign of 'anterograde Wallerian degeneration', in which gray matter pathology could be preceded by axonal dysfunction [13]. Indeed, abnormal axonal transport also has been demonstrated in AD (see review) [14]. In addition, white matter structural changes such as myelin breakdown, loss of myelin basic protein[15] as well neuroinflammation have been recognized as part of AD white matter neuropathological features[16, 17]. However in aMCI, the magnitude of white matter abnormalities is reduced compared with AD. Interestingly, neuroimaging techniques are more sensitive to detect white matter abnormalities in aMCI compared to neuropathological studies[18, 19].

The literature in aMCI overall is less extensive, however, there is an indication of its importance. As early as in 1984, Albert and colleagues showed that ventricular area measured on a CT scan discriminates AD from controls with a accuracy of 89% [20]. These findings have been extensively replicated using structural MRI. Today, ventricular volume in aMCI patients is one of the best predictors of dementia progression [21]. Ventricular dilation indicates white matter atrophy since cerebral ventricles are surrounded by white matter. As such, the study of white matter alterations in patients with a high likelihood of developing dementia is of great interest in order to understand the neurobiology of AD.

White Matter Architecture
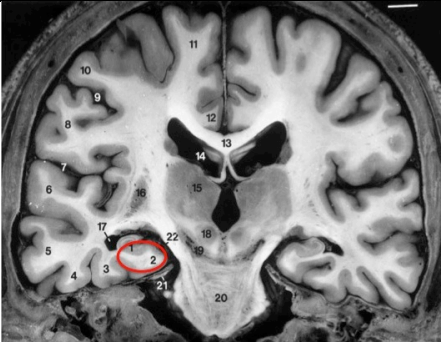
Brain white matter occupies nearly 35% of the total intracranial space [22]. White matter is organized into fascicles or bundles composed of axons connecting distinct brain areas. Axons are microscopic tubular projections of the neuronal cell bodies responsible for propagation of action potentials from the cell body to the synaptic terminals. White matter pathways connecting different segments within the central nervous system (CNS) are designated as tracts (e.g. corticospinal tract). Connections between lobes are referred to as fascicles (e.g. uncinate fascicle), and connections between hemispheres are called commissures (e.g. interhemispheric commissure). Within these white matter pathways, the parallel organization of millions of axons displays a property called anisotropy (see figure 1.1). Anisotropy (Greek for unequal direction) refers to the restricted diffusivity of cytoplasmic water parallel to the axonal fibers. Thus quantifying anisotropy allows mapping white matter pathways in the brain. Tissue anisotropy is quantified using a magnetic resonance (MR) sequence called diffusion tensor imaging (DTI), which specifically allows for *in vivo* imaging of the diffusion of water in the human brain [23]. Since the white matter of the brain is highly organized, DTI is the ideal MR technique for modeling white matter structure as well as abnormalities in neurological conditions.
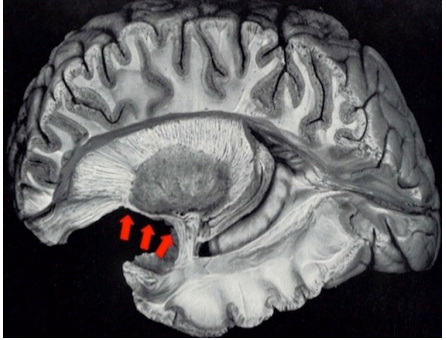
Figure 1.1: Restricted diffusion occurs parallel to the axon
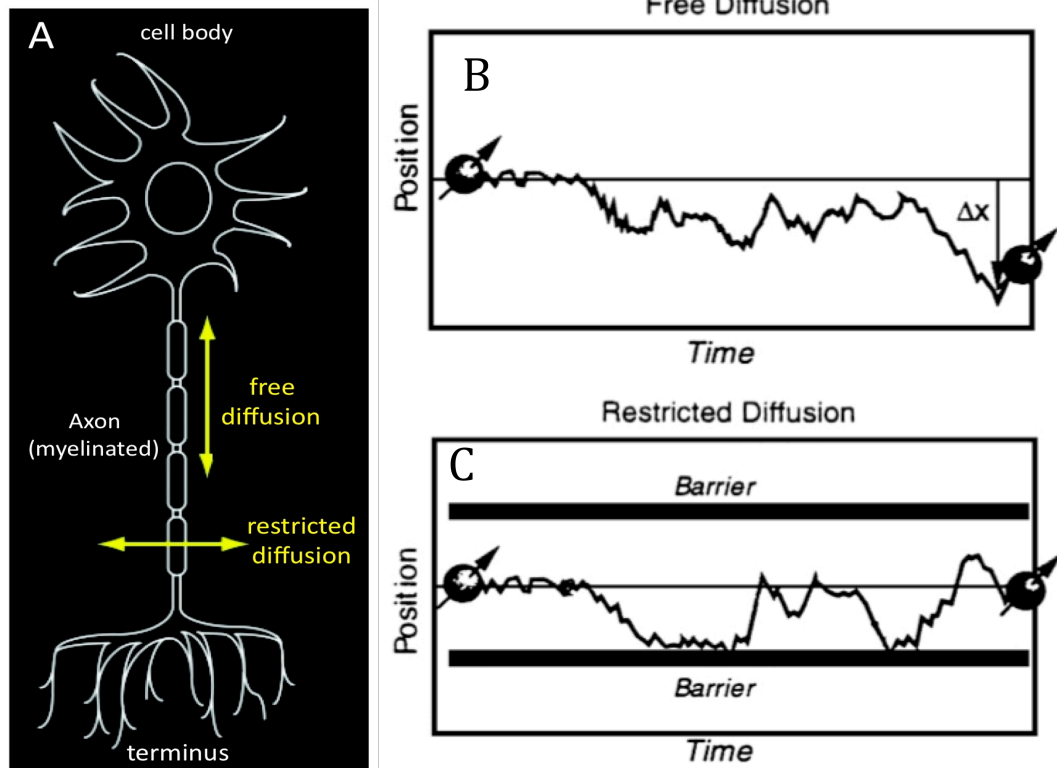
Unrestricted free diffusion of water (figure 1.1B) is prevented by the restricted diffusivity imposed by the axonal barrier (figure 1.1C). Therefore, mapping diffusivity allows determination of white matter fibers in the brain[24].

Table 1.1. White matter pathways of interest in aMCI and AD.

Anatomical Location	Pathway	Connections
	Angular bundle (Coronal view) is the white matter situated deep to the subicular complex (red). It is within this region that the perforant path fibers travel to caudal levels of the hippocampal formation. The perforant path is the most important afferent to the hippocampus.	Input to the hippocampus memory system. Fibers connecting the entorhinal cortex and the hippocampus.
	Commissural fornix (ventral view). The blue arrows indicate Topography of the dorsal hippocampal commissure. Red arrows indicate the fimbria, and the green arrows indicate the corpus callosum.	Connects the right and left hippocampal memory system.
	Fimbria and fornix (Mesial view) constitute the major outputs of the polysynaptic pathway. Empty arrows represent the fimbria. Full arrows represent the body of the fornix and orange arrows indicate the postcommissural fornix. **Anterior commissure** is an important interhemispheric commissural connection, which is represented by a light orange arrow.	Connects the hippocampal memory system to the thalamus, basal forebrain and contralateral hippocampus.

	Uncinate fascicle (Convexity view) is situated deep on the rostral part of the superior temporal gyrus and posterior to the orbital frontal cortex.	Connects the hippocampal memory system, subcallosal areas and the prefrontal lobe.
	The cingulum bundle (Mesial view) has a dorsal component that occupies the white matter of the cingulate gyrus and a ventral part situated in the white matter of the caudal part of the parahippocampal gyrus.	Connects the hippocampal memory system to the parietal, cingulate, parahippocampal cortex.
	Inferior longitudinal fascicles (Convexity view) Fibers traveling rostral terminate in the superior temporal sulcus and the lower bank of the intraparietal sulcus (red arrows). Superior longitudinal fibers (orange arrows) are also observed in this dissection.	Connects the hippocampal memory system to the occipto-temporal cortices; caudal part of the cingulate gyrus, the inferior parietal lobule.

All figures and descriptions from table 1.1 are from [25, 26].

White Matter Pathways of Interest

Memory complaints are the primary symptom of patients with aMCI; thus when studying these patients it is important to focus on the memory pathways. The hippocampal formation, which includes the hippocampus, entorhinal cortex, subiculum, pre-subiculum, para-subiculum, Ammon's horn and the dentate gyrus, constitutes the heart of declarative memory system affected in aMCI and AD [7]. Indeed the entorhinal cortex of aMCI individuals has been shown to contain phosphorylated tau and neuronal depletion as compared to healthy individuals [7]. Furthermore, in AD, neuronal depletion and intracellular inclusion further extends to the subiculum, CA1 and CA3 hippocampal fields. In fact, hippocampal formation cell depletion highly correlates with memory deficits in both aMCI and in AD [7].

In contrast to gray matter changes, degeneration to the hippocampal formation's connections have been largely overlooked in aMCI and AD research. Deafferentation following white matter lesions, is a well-known process in numerous neurological conditions [27]. Deafferentation at the level of afferent pathways feeding the hippocampal formation or output connections from the hippocampal formation to the rest of the brain, can cause memory deficits [28, 29]. White matter deafferentation at the (1) intrinsic hippocampal circuit, (2) commissural connections, (3) subcortical or (4) cortical output pathway can potentially cause amnestic syndromes, and thus are of interest in aMCI and AD research [29].

Quantification of White Matter Architecture and Integrity Using MRI

In brain imaging, white matter integrity has been quantified by diffusion acquisitions (fractional anisotropy, mean diffusivity and fiber tracking).

Mean Diffusivity

Using DTI techniques experts have developed sensitive scalar measures to quantify abnormalities within the white matter [23]. One such measure is called mean diffusivity (MD; mm^2/s). The details of this measurement are discussed in the appendix. Briefly, mean diffusivity is a measure of Brownian motion, which is typically restricted by the normal structural organization of brain tissue. MD is

increased in pathological situations characterized by damage of tissue organization such as neuroinflammation and other pathologies. In fact, numerous studies have reported increases in MD in aMCI individuals, however, the location of these abnormalities is not entirely consistent. Most studies report that MD is increased in the medial temporal lobe of aMCI individuals with some evidence that the left is more affected than the right [30-33]. However, while some studies highlight frontal, parietal and occipital lobes [34], others report the genu of the corpus callosum and the cingulate cortex are the most vulnerable regions for MD changes in aMCI patients [30, 33].

Fractional Anisotropy

Fractional anisotropy (FA; unitless) is another scalar measure of the structural organization within the brain (the details of which are outlined in the methods section). With over 2500 papers in the Pub Med database, FA is the most commonly evaluated outcome of a DTI scan; most likely do to ease of its intuitive interpretation. Like MD, there have been a number of papers evaluating the FA values of patients with aMCI and AD. Depending upon the purpose and the methodology, results vary across papers. However, FA abnormalities involving the hippocampus, entorhinal, and parahippocampal white matter are among the most commonly reported in AD [31-33, 35]. Additionally, white matter FA declines are often cited in the posterior cingulate and parietal cortex [35]. Within aMCI there has been some debate over whether or not FA abnormalities are detectable. Early papers evaluating FA in aMCI showed declines that resembled the areas reported in AD patients (same location, smaller magnitude) [36, 37]. However a number of more recent studies using a more robust registration method have been unable to detect changes in fractional anisotropy between CN and aMCI subjects [38-41].

Fiber Tracking

Fiber tractography is a method to map brain white matter pathways such as tracts, fascicles and commissures connecting brain regions. The use of diffusion tensor data to visualizing these structural tracts was first proposed by Basser [42]. Deterministic and probabilistic fiber tracking are the most common methodologies

used to investigate white matter pathways connecting two brain regions. While deterministic methods are based on the bidirectional nature of fibers, probabilistic methods provides a distribution of the probability of two points in the brain being connected. Although fiber tracking has been effectively validated in healthy individuals, its use in aMCI brains has been relatively limited.

Brain pathways outlined by deterministic fiber tractography allow fiber-specific measures of white matter organization. FA and MD abnormalities provide information regarding the impact of a disease process on a specific white matter pathway. One study focusing on memory-related white matter pathways used fiber tracking to determine their area of interest. They found abnormal FA (reduction) in the fornix and abnormal MD (increased) in the inferior and superior longitudinal fasciculus as well as the corpus callosum of patients with AD. However no abnormality was found in aMCI subjects [43]. Another study found that the total volume of fiber tracts connecting the hippocampus and the rest of the brain was reduced in AD [44]. Although deterministic fiber tractography provided significant advance of white matter abnormalities in AD and aMCI this method does not allow accurate or unbiased group comparisons, since it relies on manual placement of seed points [45]. Moreover, inability to discriminate crossing white matter pathways limits the results of deterministic fiber tractography studies [45].

Probabilistic methods, in contrast with deterministic, better deal with the uncertainty involved in fiber tracking such as crossing fibers. Preliminary work conducted in patients with AD found reductions in anatomical connectivity between the putamen and the rest of the brain as compared to healthy controls [46]. However this study didn't use optimized MRI acquisition parameters to conduct fiber tractography techniques giving them a lower signal to noise ratio as compared to the present study [46].

In summary, MRI offers a wide range of techniques to explore structural integrity of white matter projections connecting brain regions involved in neurodegenerative disease. In the case of AD and aMCI, these techniques could explore defects on the structural connectivity underlying memory circuits.

Aims and Goals

Recent advances in image acquisition (increase of image sensitivity and resolution) and methods of analysis (tractography) make DTI an ideal imaging modality for investigation of white matter connectivity in aMCI. Here, we used probabilistic fiber tractography to quantify white matter abnormalities in patients with aMCI, naMCI and AD, focusing on white matter changes in memory pathways within the temporal lobe (as these areas are primarily affected by Alzheimer's pathology) [5].

The goals of the present thesis are:

1) To quantify white matter abnormalities in naMCI, aMCI and AD individuals by examining fractional anisotropy, mean diffusivity; and

2) To create maps of hippocampal structural connectivity using probabilistic fiber tracking techniques [47, 48].

Hypothesis

1) There will be reduced FA and increased MD in both the aMCI and AD population as compared to CN subjects.

2) White matter tracts connecting areas of the brain associated with memory will have reduced hippocampal connectivity in both aMCI and AD patients as compared to CN subjects.

Chapter 2: Manuscript

Title Page

 White matter abnormalities and structural hippocampal disconnections in Alzheimer's disease and amnestic mild cognitive

Jared Rowley[1], Vladimir Fonov[4], Ona Wu[5], Simon Eskildsen[6], Dorothée Schoemaker[1], Liyong Wu[1, 2], Sara Mohades[1], Monica Shin[1], Viviane Sziklas[4], Amir Shmuel[3], Alain Dagher[3], Serge Gauthier[1] and Pedro Rosa-Neto[1, 3]; for the Alzheimer's Disease Neuroimaging Initiative*

[1]Translational Neuroimaging Laboratory, McGill Centre for Studies in Aging (MCSA), McGill University, Montreal, QC, Canada

[2]Department of Neurology, Xuan Wu Hospital, Capital Medical University, Beijing, China

[3]McConnell Brain Imaging Centre, Montreal Neurological Institute, McGill University, Montreal, QC, Canada

[4]Montreal Neurological Institute, McGill University, Montreal, QC, Canada

[5]Athinoula A. Martinos Center for Biomedical Imaging, Charlestown MA

[6]Center of Functionally Integrative Neuroscience, Aarhus University, Aarhus, Denmark

Introduction

Alzheimer's disease (AD) has been conceptualized by a succession of pathophysiological events beginning with progressive extracellular accumulation of amyloid followed by a variety of neurodegenerative changes such as intracellular accumulation of neurofibrillary inclusions, brain atrophy and cell depletion [49]. In AD, neurodegenerative changes (i.e. tau hyperphosphorylation and cell depletion) follows a typical 6-stage topographic pattern starting in the entorhinal cortex, propagating to the limbic cortex and subsequently to the polymodal association cortex [5]. In fact, the asymptomatic AD, mild cognitive impairment (MCI) and dementia stages correspond similarly to the severity of AD neuropathology propagation [5] [50].

From pathophysiological perspective, there is a growing consensus that white matter (WM) abnormalities in MCI constitute an integral part of the degenerative processes associated with AD pathophysiology. Chen and colleagues proposed that white matter pathology, as measured *in-vivo* in dementia patients, may be a sign of 'anterograde Wallerian degeneration', in which gray matter pathology could be preceded by axonal dysfunction [13]. WM structural changes such as myelin breakdown, loss of myelin basic protein[15], neuroinflammation as well as abnormal axonal transport have been recognized as part of AD WM neuropathological features [16, 17,14].

The role of WM degeneration in AD has been explored in vivo with Magnetic Resonance Imaging (MRI; see review [51, 52]). Mean diffusivity (MD) and fractional anisotropy (FA) are MRI diffusion tensor imaging (DTI) outcome measures informative of microstructural organization of water in WM compartments. High MD conveys local increase of free water diffusivity in WM, which possibly is linked to reduction in myelin content, axonal depletion or declines on extracellular matrix [53]. Low FA indicates loss of diffusion directionality, which is imposed by abnormal axonal membranes. In fact, post mortem data show a correlation between FA axonal and myelin WM contents [53]. Advances in image processing allow the estimations of WM pathways, which are derived from Bayesian mathematical models (probabilistic

tractography) [54]. These techniques provide a metric to estimate the degree in which WM abnormalities disrupt long pathways connecting distinct brain regions. Thus, assessment of WM abnormalities using MRI can expand classic neuropathological approach by estimating WM structural connectivity in major WM pathways [18, 19].

MCI due to AD is a condition characterized by objective cognitive deficits which minimally interfere with activities of daily living [3]. Peterson and colleagues outlined a classification of MCI as amnestic mild cognitive impairment (aMCI) and non-amnestic mild cognitive impairment (naMCI), based on the predominance of memory deficits over other cognitive domains [11]. It has been established that local WM disconnections between the entorhinal cortex and hippocampus (i.e. perforant path) are involved in AD and MCI pathophysiology, however large-scale hippocampal WM connectivity has never been systematically assessed in these populations [9, 55]. Large-scale hippocampus structural connectivity indicates the severity of disconnections between limbic and polymodal association cortex. Here, we aimed to compare patterns of brain FA and MD abnormalities as well as hippocampal connectivity among aMCI, naMCI and AD individuals. We hypothesized that there will be greater severity of MD and FA abnormalities in AD. In addition, we predict disconnections on large-scale hippocampal WM networks in aMCI and AD.

Methods

Two cohorts were analyzed in this study. The first cohort of aMCI and cognitively normal (CN) individuals was recruited at the McGill Centre for Studies in Aging (MCSA cohort) located in Montreal, Quebec, Canada. An independent cohort of CN, MCI (classified into aMCI and naMCI), and AD was obtained from Alzheimer's Disease Neuroimaging Initiative Go /2 (ADNI cohort). Informed consent was obtained from each subject in accordance with local institutions' Research Ethic Boards (REB) [56]. The McGill University Research and Ethics committee approved these protocols.

MCSA Cohort Data Acquisition

The McGill Centre for Studies in Aging (MCSA) staff was responsible for patient recruitment, screening and enrollment in the MCSA cohort. Patients with

subjective memory complaints, substantiated by a knowledgeable informant were clinically assessed (SG). Subsequently, patients underwent a full medical, neurological examination and battery of neuropsychological tests including the standard Mini Mental State Examination (MMSE) and Rey Auditory Verbal Learning Test [57]. Diagnosis of aMCI was achieved by a consensus in a clinical diagnosis meeting based on the Peterson criteria [11].

Age and gender matched controls enrolled in this study, referred here as CN, were recruited by advertisements in local newspapers. CN exclusion criteria were (1) presence of current or past neurological or psychiatric condition and (2) history of memory complaints. Exclusion criteria for all subjects included a history of psychological problems, intellectual inability, past psycho stimulant drug use or brain vascular lesions on the Fluid attenuation inversion recovery (FLAIR) MRI.

MRI data was acquired on a Siemens 3T Trio MR scanner (Siemens Medical Systems, Erlangen, Germany) using a 32-channel phased-array head coil. Diffusion encoding was achieved using a single-shot spin-echo echo planar sequence with twice-refocused balanced diffusion encoding gradients. High angular resolution reconstruction was acquired with 99 diffusion encoding and 10 resting (b0) directions, 2mm isotropic voxel size, 63 slices, b=1000 s/mm², TE=89ms, TR=8.3s. A 1mm isotropic resolution T1-weighted anatomical scan was also acquired (TR=18ms, TE=10ms, FA=30 degrees). The two datasets were registered using a mutual information based algorithm [58] to remove image misregistration from echo planar induced image shifts and motion. All scans were conducted at the Montreal Neurological Institute.

ADNI Cohort Data Description

A second dataset used in the preparation of this article was obtained from the Alzheimer's Disease Neuroimaging Initiative (ADNI) database (adni.loni.ucla.edu). The ADNI was launched in 2003 by the National Institute on Aging (NIA), the National Institute of Biomedical Imaging and Bioengineering (NIBIB), the Food and Drug Administration (FDA), private pharmaceutical companies and non-profit organizations, as a $60 million, 5-year public-private

partnership. The primary goal of ADNI has been to test whether serial magnetic resonance imaging (MRI), positron emission tomography (PET), other biological markers, and clinical and neuropsychological assessment can be combined to measure the progression of mild cognitive impairment (MCI) and early Alzheimer's disease (AD). Determination of sensitive and specific markers of very early AD progression is intended to aid researchers and clinicians to develop new treatments and monitor their effectiveness, as well as lessen the time and cost of clinical trials.

The Principal Investigator of this initiative is Michael W. Weiner, MD, VA Medical Center and University of California – San Francisco. ADNI is the result of efforts of many co-investigators from a broad range of academic institutions and private corporations, and subjects have been recruited from over 50 sites across the U.S. and Canada. The initial goal of ADNI was to recruit 800 subjects but ADNI has been followed by ADNI-GO and ADNI-2. To date these three protocols have recruited over 1500 adults, ages 55 to 90, to participate in the research, consisting of cognitively normal older individuals, people with early or late MCI, and people with early AD. The follow up duration of each group is specified in the protocols for ADNI-1, ADNI-2 and ADNI-GO. Subjects originally recruited for ADNI-1 and ADNI-GO had the option to be followed in ADNI-2. For up-to-date information, see www.adni-info.org.

From the ADNI-GO and ADNI-2 dataset, we selected all participants aged 55 to 90 years of age (inclusive) who had completed, during the course of a single visit, the following clinical, imaging and neuropsychological assessments: T1 MRI, DTI, Mini Mental State Examination (MMSE), Clinical Dementia Rating scale (CDR), Wechsler Memory Scale Logical Memory II, Alzheimer's disease assessment scale (ADAS)-cog, Rey auditory verbal learning test (RAVLT). Selected individuals were classified as CN, MCI (divided into aMCI, naMCI) and AD, on the basis of clinic-behavioral measures put forth by ADNI.

The data was acquired from 14 centers around the USA and Canada between 2010 and 2012. The scanning parameters were as follows. All diffusion images were scanned on GE 3 tesla scanners. There were 41 diffusion encoding and 5 resting (b0) directions, 1.4mm x 1.4mm x 2.7mm voxel size, b=1000 s/mm². All scans used were

already EPI-eddy current corrected by ADNI. T1 scans were acquired on the same GE 3T scanner with a 1.2 mm x 1mm x 1mm voxel size. Further acquisition details are available from ADNI website (ADNI-INFO.org)

Clinical Operational Definitions

The criteria for CN included an MMSE score ranging between 24-30 (inclusive), and a CDR score of 0 [59, 60]. ADNI2 and ADNIGO define MCI as individuals with subjective memory complaint, an MMSE score between 24-30 (inclusive), objective memory loss as shown on scores on delayed recall of one paragraph from the Wechsler Memory Scale Logical Memory II, a CDR of 0.5, preserved activities of daily living, and the absence of dementia [61, 62].

We reclassified ADNI MCI individuals in aMCI or naMCI as defined as 1.5 std. below CN on 30 min auditory verbal learning test (AVLT) delay recall [63]. In addition to the NINCDS/ADRDA criteria for probable AD, mild AD dementia subjects had MMSE scores between 20-26 (inclusive) and a CDR of 1 [64].

T1 Processing

Individual T1 MRIs were skull stripped [65], non-uniformity corrected [66] and registered to MNI152 space nonlinearly [67]. The T1 was then classified into grey matter, white matter, and cerebrospinal fluid with a validated automated classification algorithm [68] and subsequently automatically labeled using Automatic, Nonlinear, Imaging Matching and Anatomical Labeling (ANIMAL)[69]. Individual segmented hippocampus was used as a seed region for the hippocampal structural connectivity (HSC).

DTI Processing

FA and MD maps were generated using FSL-DTIFIT from the skull-stripped [70] eddy current corrected images in MRI native space.

HSC Processing

HSC maps were generated using a pipeline based on FSL 4.1-FDT (Figure 1). In brief, (1) DTI images were skull-stripped using BET2 and Eddy current-corrected [71] ; (2) At each voxel of individual DTI images, a probability distribution of fiber direction was generated using FSL-bedpostx with a maximum of two fiber directions

per voxel [72] ; (3) single voxel level probabilistic maps were generated for every voxel of the seed region using FSL-probtrackx (approx. 400 maps per region; see animation in the supplementary materials). These maps represented the probability that any given voxel in the brain was connected to a seed voxel. Finally (4) a single HSC map of the entire hippocampus was computed via the max function derived from the single voxel level maps. Thus a given voxel value in the HSC map represents the likelihood of this voxel being connected to the hippocampus. HSC maps were generated with seed regions in both the left and right hippocampus.

DTI Statistics

FA, MD and HSC statistical group differences were created using the track-based spatial statistic tool (TBSS) [73]. Firstly, all FA images were aligned to the MNI 152 standard space [74]. Then a skeleton was created from the mean FA > 0.2. Local maxima of FA images of each subject were then projected onto the skeleton. At each voxel in the skeleton statistical group differences were determined using permutations tests (FSL randomize) [75]. MD and HSC maps were projected onto the same skeletons to determine statistical group differences. The statistical results were thickened to allow better visualization of group differences. Correction for multiple corrections was estimated using family wise error (FWE) and the threshold-free cluster enhancement (TFCE) option [75]. Additionally, global averages for FA and MD were calculated for each subject using the WM skeleton as a ROI. To estimate the normalized abnormal MD or FA volumes, we computed the ratio between the volume of abnormal voxels when compared to CN as defined by TBSS (corrected $p < 0.05$) and the total WM skeleton volume.

Results

Demographics

In the MCSA cohort an unpaired one-tailed t-test showed that CN and aMCI groups did not differ in terms of gender, age, and educations (table 1a). As expected, MMSE, RAVLT, and APOE status was different between groups.

In the ADNI cohort a 1-way ANOVA of the ADNI demographics showed the CN, aMCI, naMCI and AD groups did not differ in terms of gender, age, and education

(table 1b). Post-hoc comparisons using Tukey's HSD indicated significant differences in MMSE, AVLT, and APOE status. There was no demographic difference between the aMCI group and the naMCI group other than the AVLT score.

DTI Outcome Measures

Average FA and MD values are represented in figures 2A and 2B. Note that global average FA and MD were significantly different between cohorts. Figure 3A shows the average HSC obtained in the CN, depicting patterns of hippocampal connectivity known from experiments obtained in post mortem tissue, such as projections to the entire temporal neocortex as well as to cingulate cortex as well as associative parietal occipital and frontal cortices.

DTI Group Differences

In the MCSA aMCI cohort, 29% of normalized WM volume had significantly elevated MD compared to the CN group. Corpus callosum, arcuate, uncinate, superior and inferior longitudinal fascicles were affected (Figure 4A). Voxels with abnormal MD in aMCI were on average 7.1% higher than CN (Figure 2B). Global WM MD was elevated 5.5% in aMCI (p=0.003) compared to CN. None of the clusters of reduced FA were significant after correcting for multiple comparisons. HSC revealed no hippocampal connectivity abnormalities in aMCI.

In the ADNI cohort (Figure 4B) **aMCI (aMCI>CN)** showed abnormal mean diffusivity in 27.6% of normalized WM volume, particularly on the corpus callosum, splenium, superior and inferior longitudinal fascicles, and arcuate fascicles. These abnormal voxels had an average of 5.8% higher MD than CN. Global WM MD was elevated 4.1% in aMCI compared to CN (p=0.039) (Figure 2B). Similarly to the MCSA cohort, ADNI aMCI had no significant declines in FA. No WM abnormalities were observed in the reverse statistical comparison [aMCI< CN]. No hippocampal connectivity abnormalities were observed in aMCI.

In naMCI, part of ADNI cohort, neither FA nor MD values differed from CN.

The **AD** patients in the ADNI cohort (Figure 4C) showed abnormally elevated MD in 66.3 % of normalized WM volume compared to CN. These abnormalities were observed particularly in the genu and splenium of the corpus callosum, uncinate,

superior and inferior longitudinal fascicles and cingulate bundle. Abnormal voxels in these pathways had an average of 8.5% higher MD than CN. Global WM MD was elevated 7.1% in AD (p=0.0001) (Figure 2B). In addition, FA was abnormally low in 54.3% of the normalized WM volume. In these abnormal voxels, FA was 11.3% lower than CN. Interestingly, 75% of WM regions with abnormally lower FA also had abnormally higher MD. Global WM FA was reduced by 7.9% (p=0.0004) (Figure 2A). No FA elevations or MD declines were observed in AD.

HSC showed reduced hippocampal connectivity (Figure 3B and 5) in the temporal lobe (angular bundle, inferior longitudinal and uncinate fascicles), limbic projections (cingulate bundle and fornix), inferior parietal cortex (arcuate fascicles) and frontal (occipito-frontal and superior longitudinal fascicles) in AD patients compared to CN. All other contrasts were not significant after correcting for multiple comparisons.

The contrasts between **AD and naMCI** patients of the ADNI cohort revealed abnormally high MD in 54% of AD normalized WM volumes (Figure 4D). Abnormal normalized WM volume in AD had an average of 7% higher MD than naMCI. Global WM MD was elevated 5.2% in AD as compared to naMCI (p=0.001) (Figure 2B). In comparison with naMCI, AD patients had abnormally reduced FA in 57.7% of the normalized WM volume. These abnormal voxels had an average of 10.6% lower FA in AD in comparison with naMCI. Global WM FA was reduced by 6% (p=0.003) in AD in comparison with naMCI (Figure 2A).

The **AD to aMCI** contrast of the ADNI cohort (Figure 4A) revealed no abnormal MD voxels after correcting for multiple comparisons. Global WM MD was elevated 3.5% in AD as compared to naMCI (p=0.047), however this was just barely significant. FA was abnormal in 0.34% of the normalized WM voxels. Abnormal voxels had 12.5% lower FA than CN. Global WM FA was reduced by 5.3% (p=0.03) (Figure 2A).

Both FA and MD values in ADNI cohort, showed no abnormalities in naMCI (aMCI vs. naMCI) after correcting for multiple comparisons.

Discussion

Brain WM forms the backbone of a large network connecting multiple segregated cortical regions, which occupies nearly as much of brain volume as the gray matter [76]. There is a growing body of the literature suggesting active WM degeneration as part of the repertoire of pathophysiological process underlying AD. Although neglected, the impact of WM abnormalities in AD has been reported to be large [13, 19, 53].

Here, we report increased MD (6-7%) occurring in approximately 28% of normalized WM volume and no FA declines in aMCI. In contrast, the WM of AD individuals had higher MD (8.5%) and lower FA (11.3%) affecting a larger proportion (66%) of normalized WM volume. The magnitudes of MD or FA group differences reported here are above expected variability as revealed by several DTI test-retest studies [77]. In addition, we report, for the first time, the deleterious effects of WM abnormalities in the hippocampal connectivity of AD patients using the FSL's probabilistic tractography method [54]. This technique provides the likelihood of connectivity between the hippocampus and any given brain region. Our results support the hypothesis that AD brain undergoes a progressive WM degeneration characterized firstly by increased MD, followed by declines in FA and reduction of hippocampal connectivity.

The modest but significant increase of MD found in aMCI (both MCSA and ADNI cohorts) supports the construct that increased WM water diffusivity constitutes an early neurodegenerative event associated to AD pathophysiological processes. Although high MD has been frequently reported in aMCI populations [39, 41], there has been some disagreement. For instance, Agosta and colleagues only found widespread changes in axial diffusivity but no significant MD differences in 15 aMCI individuals [38], however, this disparity could be explained by the both fact they were using a 1.5 T MRI and had lower in-plane resolution.

Increase of tissue water diffusivity, measured as $m^2 \bullet s^{-1}$, might occur due the reduction of tissue barriers imposed by various causes (i.e. tissue atrophy, neuroinflammation), however empirical evidence supporting this claim is undermined by effects of tissue fixation typically utilized in post-mortem / DTI

correlation studies [53]. Absence of FA reduction in aMCI, as reported here, is consistent with previous studies using similar methodology (i.e. same MCI inclusion criteria, 3T acquisitions and strict TBSS analysis) [38-41]. Interestingly, evidence suggests that aMCI patients 10 years older than those in the present study have present brain regions displaying abnormal FA [78].

Two previous studies focusing on FA and MD abnormalities in naMCI provide conflicting results [41][78]. In fact, older age and the presence of multiple pathologies could account for these conflicting results [78].

The two-fold increase of normalized WM volume showing increased MD in demented patients (as compared to aMCI) supports the hypothesis that WM pathology also progresses in AD. Higher normalized WM volume showing lower FA in demented individuals in comparison with aMCI or naMCI further corroborates WM progressive degeneration in AD. In fact, progression of WM abnormalities has been previously suggested by cross sectional and longitudinal DTI studies [39-41, 79]. As a whole, these studies suggest increases of MD as an early WM degenerative event in AD.

In addition to the Wallerian degeneration originating in cortical cell bodies, recent advances in pathophysiological mechanisms underlying FA and MD abnormalities described in AD can be partially attributable to independent WM neurodegeneration. A growing body of literature suggests that WM DTI abnormalities might be secondary to neuroinflammatory factors [80]. Corroborating this hypothesis, imaging studies with PET and molecular imaging agents show increase of microglia activation and astrocytosis in the WM of aMCI [81-83]. In addition, it is noteworthy that ventricular enlargement (a surrogate of WM atrophy) is able to accurately distinguish between MCI and AD and has been proposed as tool for measuring disease progression in the short term [84].

We also demonstrated hippocampal WM connectivity abnormalities in AD dementia. Hippocampal connectivity abnormalities affected hippocampal connections predominantly to the temporal, parietal, occipital and frontal polymodal associative areas (Figure 5). The structural connectivity outcome measure described here (HSC) represents the probability of a given brain area to be

connected with the hippocampus. WM areas with significant decline of probability to be connected to the hippocampus were interpreted as depleted from normal hippocampal connectivity. The results from our HSC CN maps are in excellent agreement with the post-mortem data describing hippocampal connectivity [85]. Individual connectivity maps generated by this study in CN captured the classical reciprocal hippocampal connections with temporal, cingulate, inferior parietal and frontal cortices. Since the nature of DTI does not permit the inference of directionality, one cannot discriminate between hippocampal-petal and hippocampal-fugal fibers. Areas with reduced structural connectivity revealed by the HSC technique in AD was consistent with functional disconnections frequently reported by the literature. For example, low hippocampal connectivity in the cingulate bundle might explain functional disconnection reported between the hippocampus and the posterior cingulate / precuneus frequently described by numerous AD rsfMRI studies [86, 87]. Moreover, the WM connectivity reduction of the arcuate fascicles, inferior longitudinal and uncinate fascicles and superior longitudinal fascicles is a possible mechanism underling the $[^{18}F]$ FDG signature of AD (hypometabolism in the posterior cingulate, inferior parietal, temporal and prefrontal cortices) [88]. Hippocampal WM disconnections as described here corroborate the theoretical framework that emphasizes cortical disconnections as a key feature of AD [89]. In fact, neuropathological, functional neuroimaging and neuropsychological evidence indicate WM disconnections as a pathophysiological mechanism involved in AD.

The relative integrity of hippocampal connections in aMCI or naMCI, as predicted in our hypothesis, is supported by histopathology evidence showing tangle pathology and WM disconnection affecting predominantly transentorhinal projections to the dentate gyrus (perforant path) in aMCI, while projections from the hippocampus and subiculum and the rest of entorhinal cortex are affected in more advanced stages of the disease [5]. Possibly, a seed point in the transentorhinal cortex could better capture perforant path depletion in aMCI stage, however transentorhinal connectivity is beyond the scope of this specific study.

Limitations

Some methodological issues limit the interpretations of the present results. Since this is a cross sectional study, inferences regarding progression of WM pathology in the spectrum of AD clinical manifestations are speculative. The hypothesis posing MD increases as an early WM AD pathophysiology change followed by FA declines should be assessed by appropriate longitudinal studies.

Vascular pathology is certainly a potential confounder in all studies of this nature, since vascular insults and small vessel disease constitute a frequent finding in the MRI of elderly populations. For example, white matter intensities detected in T2 or FLAIR images may have an impact on various DTI outcome measures. However, since all patients recruited in this study, had Hachinski scores lower than 4, the impact of these lesions are not clinically significant. Particularly on the MCSA cohort, the presence of white matter intensities was minimal and monitored with 3D FLAIR MRI. Since the results obtained from the MCSA and ADNI cohorts were identical, it seems that vascular pathology affects these two populations in a similar fashion.

Although ADNI provides a powerful database for AD research, the drawback of utilizing DTI acquisitions acquired in 14 different scanners might represent a limitation for this study. While there were large efforts taken to cross-validate MRI scanners, multiple scanners acquisition is an undeniable confounding factor.

Regarding statistical analysis, TBSS is a conservative but extensively utilized method to compare WM change in numerous experimental populations [41, 90, 91]. Particularly in the case of this study, the results using voxel-based non-parametric statistics provide similar results to TBSS (data not shown). Analytical protocols can potentially constitute a bias particularly for those studies utilizing voxel-based parametric statistical analysis without correcting for multiple comparisons.

In conclusion, we found in aMCI WM abnormalities are characterized by high MD, which are possibly secondary to brain inflammatory changes or WM axons or myelin content depletion. Furthermore, the concomitance of MD and FA abnormalities observed in AD suggests higher degree of WM microstructural lesion, which impacts in large-scale brain structural connectivity. Further longitudinal

studies are necessary to corroborate whether a progression of WM disease occurs in the spectrum of clinical manifestation of dementia.

Tables and Figures

	MCSA Cohort		ADNI Cohort			
	CN	**aMCI**	**CN**	**aMCI**	**naMCI**	**AD**
N	15	19	25	21	47	15
Gender (M/F)	7/8	8/11	13/12	12/9	29/18	9/6
Age (years)	67±5.7	71.6±8.2	73.3±5.5	73.3±6.9	73.4±7.7	75.7±11.3
Weight (kg)	76±12.6	64.9±12.4	79.9±14.4	76.3±11.6	79.3±13.5	76±15.9
Education (years)	15.3±2.9	14.11±3.4	16.2±2.7	16.3±3	16.2±2.6	16±2.8
MMSE	29.2±1.1	25.9±2.4*	$28.9\pm1.5^{b,d}$	$27.7\pm1.3^{a,d}$	28.2 ± 1.5^{d}	$23.3\pm1.8^{a,b,c}$
RAVALT/AVLT	9±2.1	4±3*	$12.9\pm1.6^{b,d}$	$6.7\pm1.4^{a,c}$	12.6 ± 1.7^{d}	$5.4\pm4.3^{a,c}$
APOE (carrier/n)	1/8	7/10	4/13	6/10	15/41	4/6

A   B

Table 2.1: Demographics

Summary of Demographic and memory scores for all groups in the ADNI and MCSA cohorts.

-> t-test in the MCSA cohort revealed significant difference (p>0.05).Post-hoc Tukey HSD tests is indicated by abbreviations. a -> significantly different (p<0.05) when compared to CN. B -> significantly different (p<0.05) when compared to aMCI. c -> significantly different (p<0.05) when compared to naMCI. d -> significantly different (p<0.05) when compared to AD.
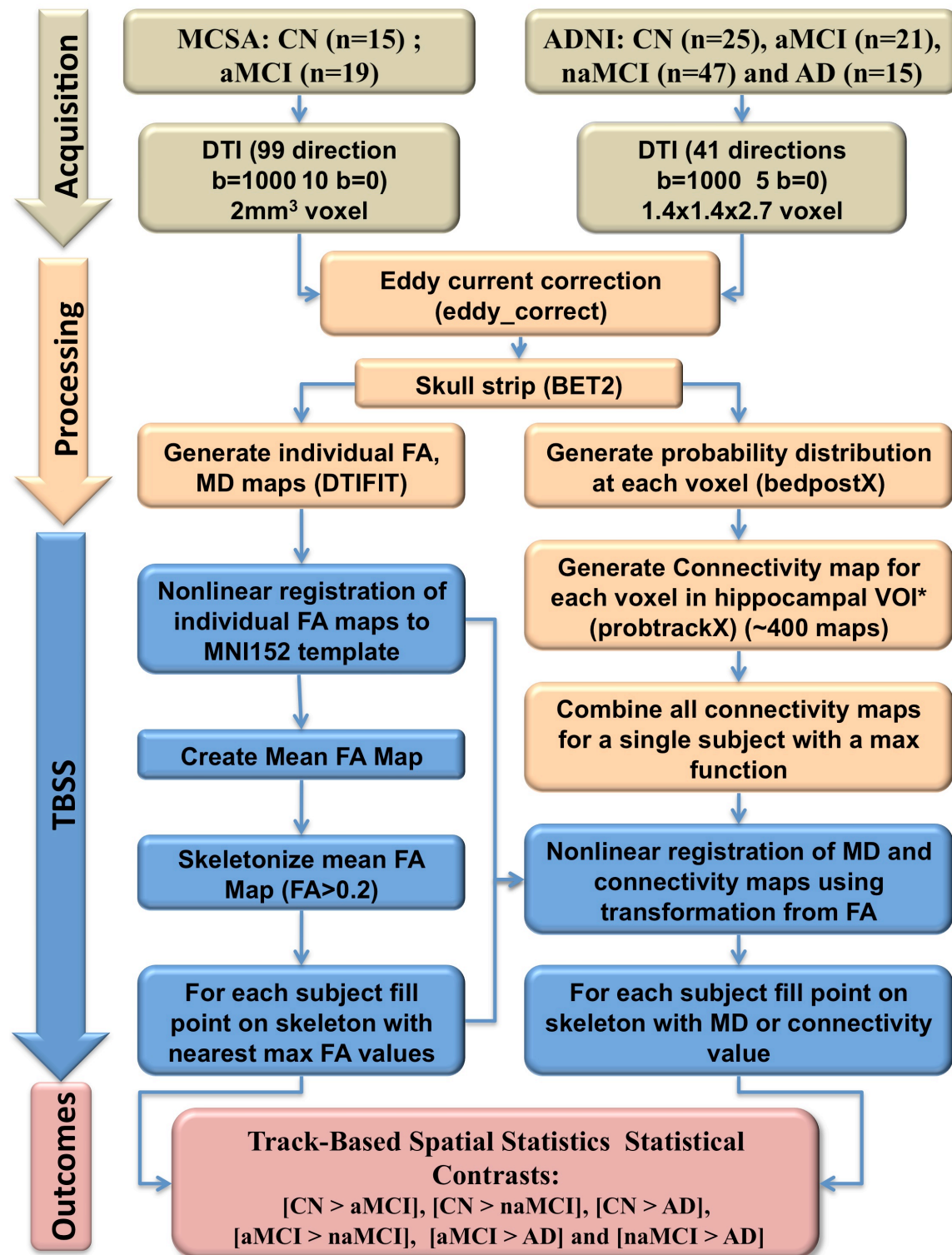
Figure 2.1: Summary Imaging Analysis Pipeline.
*Hippocampal VOI was estimated using individualized brain segmentations.
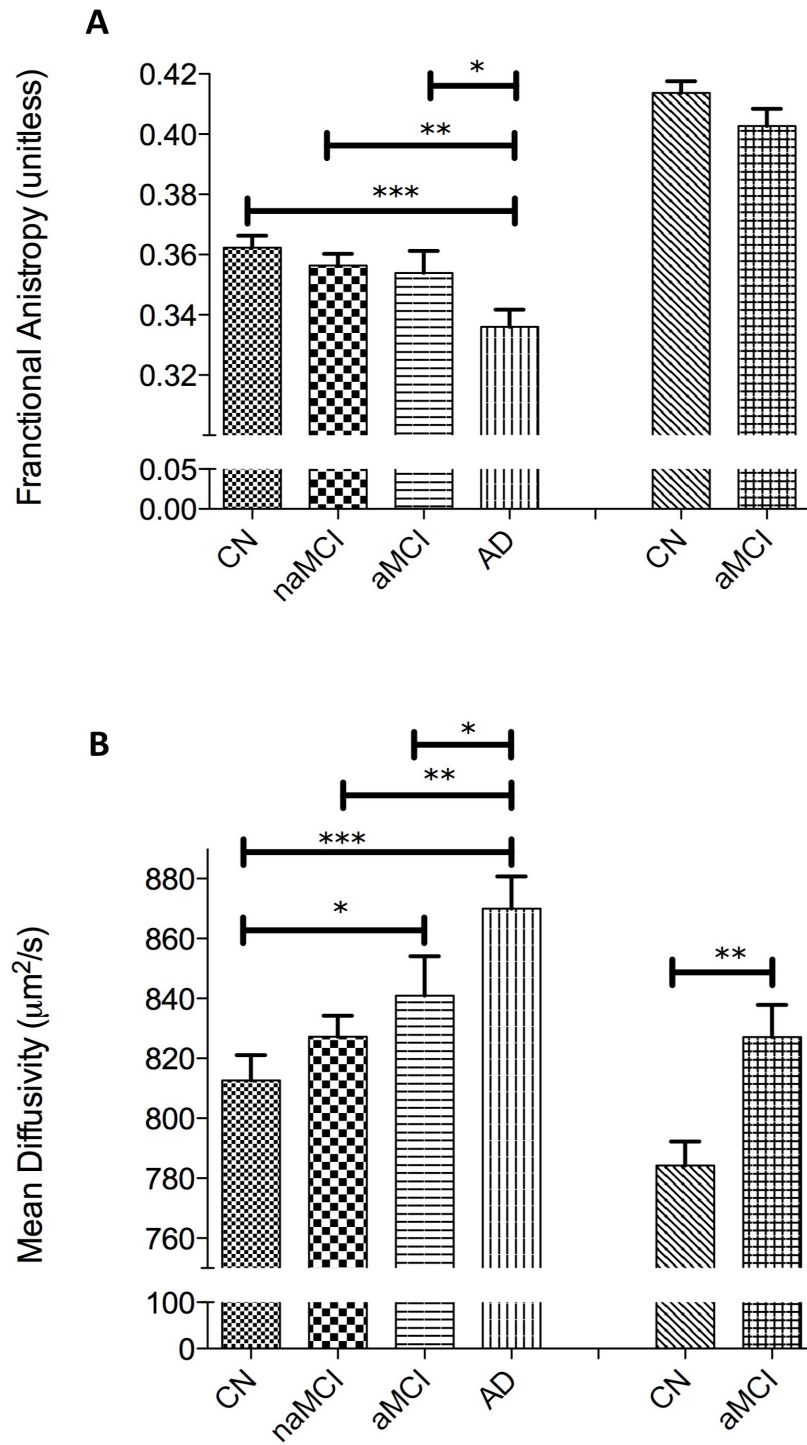
Figure 2.2: Global FA and MD Statistics
Global FA (A) and MD (B) values by group. The 4 columns on the left are from the ADNI cohort and the 2 on the right are from the MCSA cohort. *p<0.05 **p<0.005 ***p<0.0005
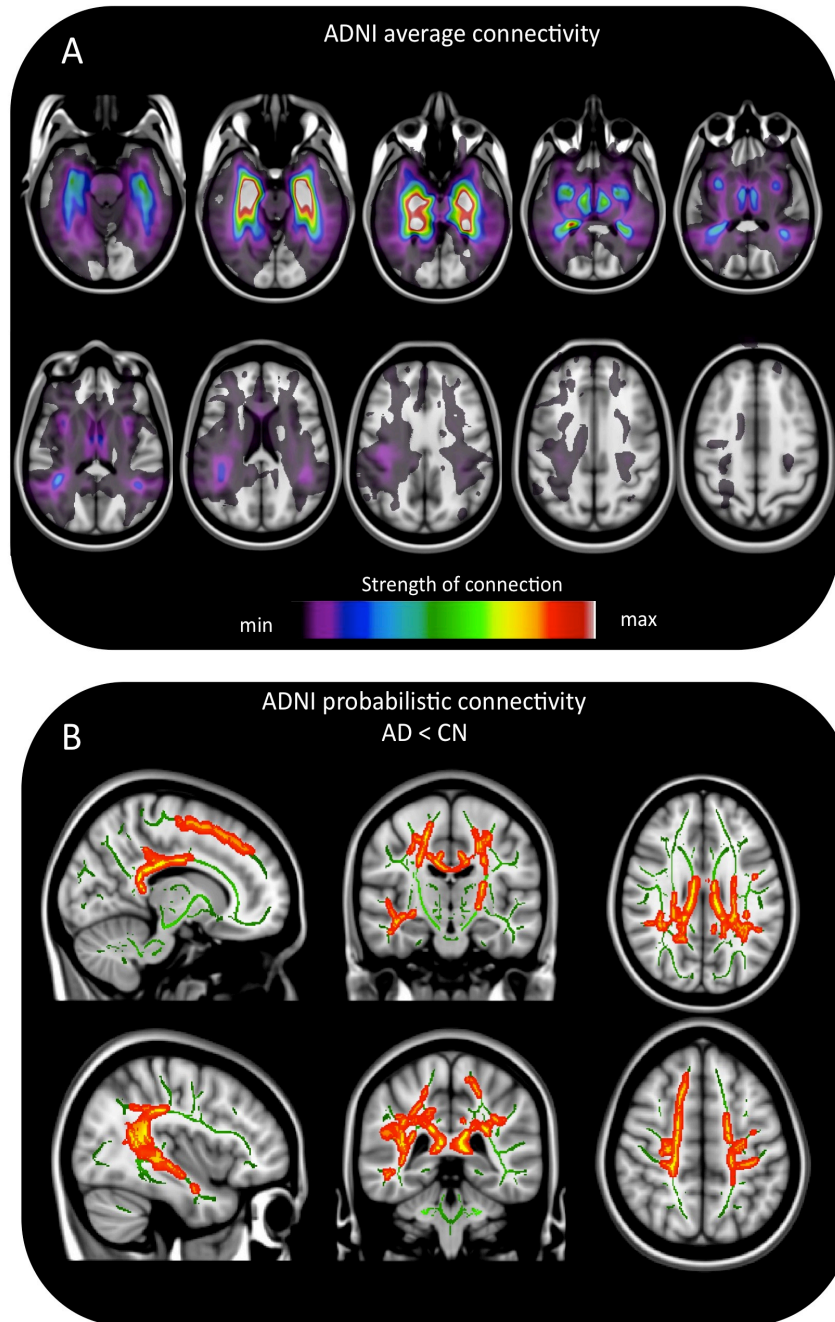
Figure 2.3: Connectivity Volume Space
Average hippocampal structural connectivity (A) for the CN group. Statistically significant reduction of connectivity is observed in AD as compared to CN (B). Note connectivity reduction on angular bundle, fornix, superior longitudinal, inferior longitudinal, cingulate, uncinate and arcuate fascicles.
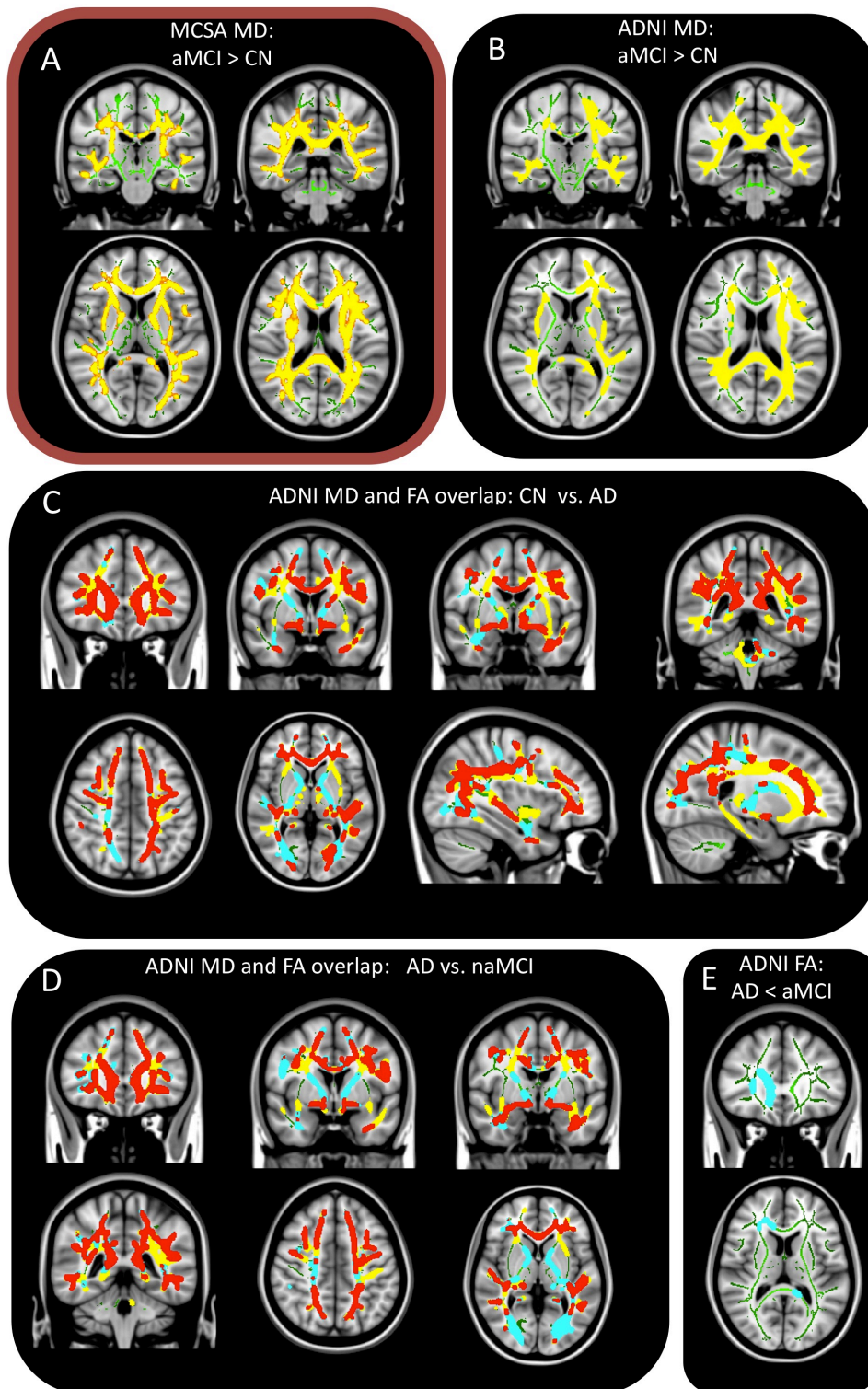
Figure 2.4: FA and MD Group Differences

Statistically significant group differences of MD (yellow), FA (blue). Notice figure C and D

show overlap of MD and FA in red. Contrasts not shown were not significant.
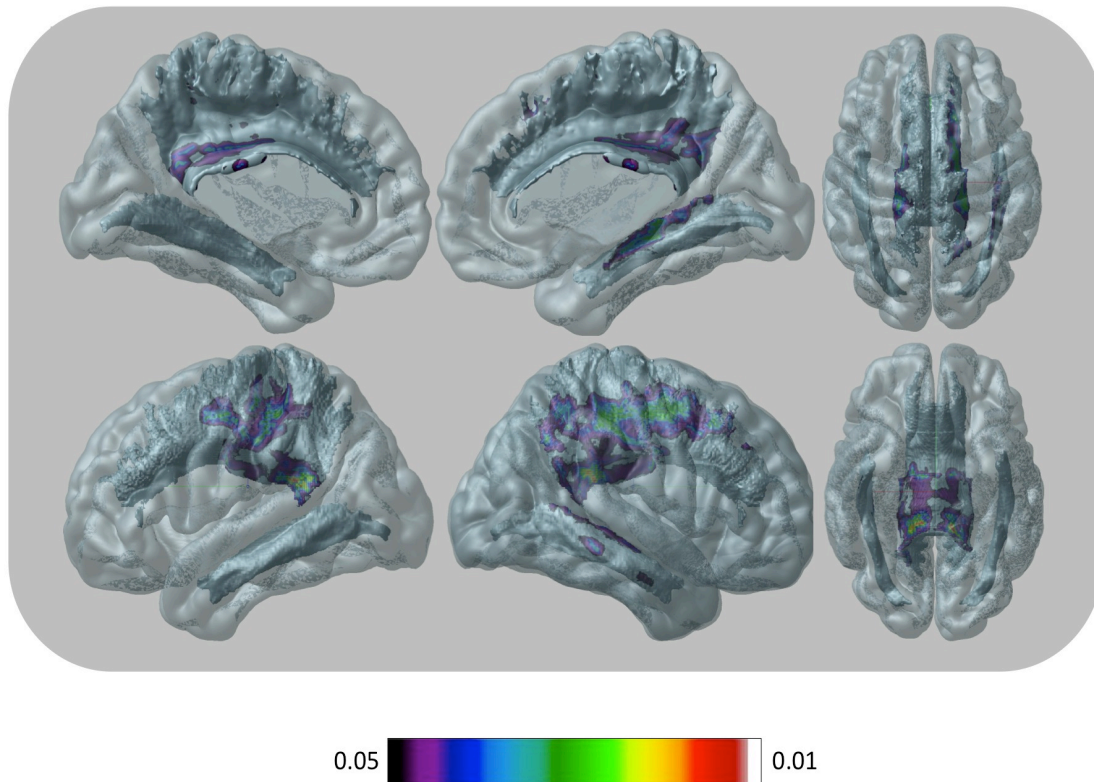
Figure 2.5: Connectivity Statistics Surface Space

Areas of reduced connectivity in AD projected on WM pathways on surface space. Note connectivity reduction on angular bundle, fornix, superior longitudinal, inferior longitudinal, cingulate, uncinate and arcuate fascicles. (See animation http://www.youtube.com/watch?v=LuRgO0I4TZU).

Chapter 3: Summary, Conclusions, and Future Directions

While Alzheimer's disease is classically viewed as a gray matter disease, here, using two independent cohorts, we were able to show white matter abnormalities in patients with aMCI and AD. The white matter of the brain is composed of highly organized tracts of myelinated axons that connect distinct cortical areas [26]. Cortical areas connected by white matter tracts form complex brain networks, which subserves normal cognitive function. From a simplified perspective, disruption of these connections could lead to cognitive dysfunctions by disconnecting cortical regions.

The results presented in this thesis indicate WM abnormalities in AD. In two independent cohorts of aMCI subjects, we demonstrated increased water diffusion within white matter tracts associated with memory circuits. A more extensive and severe increase in water diffusivity could be seen in the AD patients. We found no significant declines in fiber directionality in either aMCI population when compared to CN but did find significant declines in the AD population. Together, these findings suggest that while increased water diffusivity constitutes an early abnormality, fractional anisotropy declines represent a later event in AD pathophysiology.

Finally, as expected, we found reduced hippocampal structural connectivity in patients with AD as compared to CN but not in aMCI or naMCI groups. Differently from fMRI connectivity, structural connectivity indicates deterioration of white matter bundles connecting the hippocampus with the entire brain. The presence of disconnections in the AD but not aMCI or naMCI suggests that hippocampal connectivity as measured by probabilistic fiber tractography occurred later in the AD pathophysiological evolution.

The current framework of biomarker cascade of AD pathophysiological events (Jack's curves) has been recently updated [92]. The revised Jack's curve now incorporates conceptual changes such as biomarker sensitivity, assuming that Alzheimer's disease pathophysiological process starts years before it is detectable by current biomarkers. Moreover, Jack's curve also incorporates a hypothetical

timeline of when different biomarkers of Alzheimer's can be detected using current techniques. Specifically CSF Aβ_{42} is the first to be detected followed by amyloid PET, CSF tau, MRI and finally cognitive impairment [92]. This comprehensive model, depicted in figure 3.1, has been widely cited as a summary of current research into Alzheimer's disease. The horizontal line, labeled 'detection threshold,' signifies the level of abnormality that must exist before detection is present. Based on the evidence presented here we would like to suggest that white mater abnormalities could occur between CSF-tau and [^{18}F]FDG changes (represented in the plot as the yellow shade). The focus of the thesis was not to compare biomarkers so it is difficult to speculate where exactly the DTI curve should be placed.
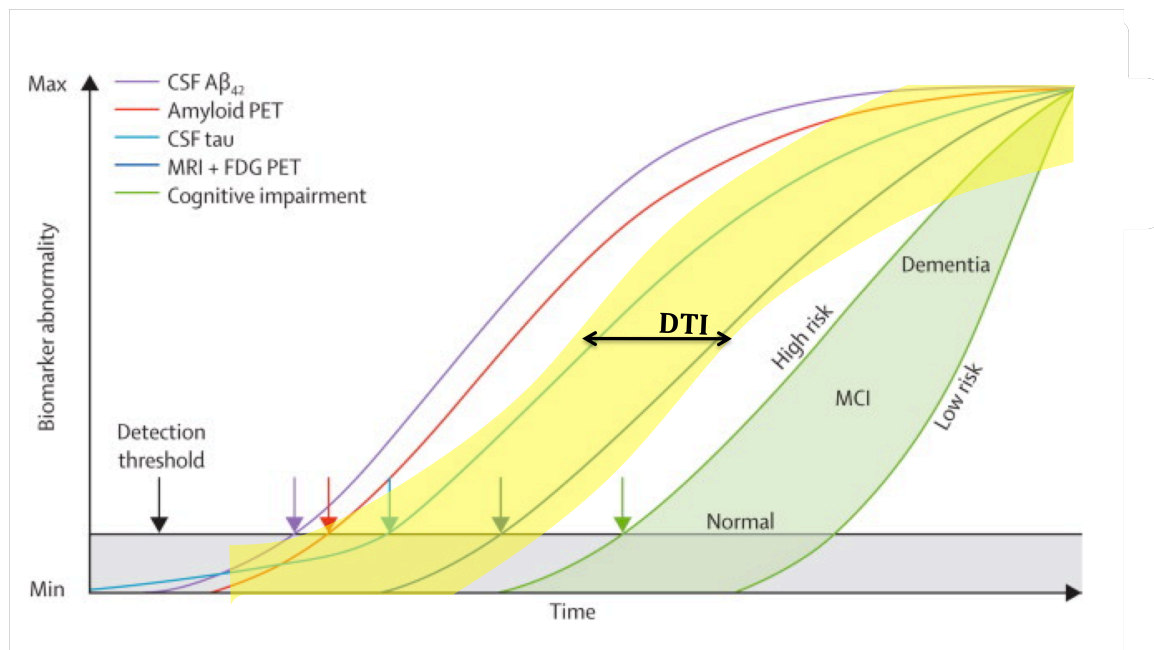
Figure 3.1: hypothetical model of dynamic biomarkers in AD
Figure adapted from Jack et. al. [92] to include a hypothetical curve representing DTI.

Future Directions

As the population ages the incidence of Alzheimer's is expected to grow [2], exacerbating the need for effective treatment. Preclinical diagnosis of Alzheimer's disease using biomarkers will certainly expand therapeutic opportunities for testing novel treatments. Current research methods have identified a number of markers

for diagnosis of preclinical AD [93, 94], but none of these methods are able to predict with high accuracy the development of the disease at the individual level. Development of these prognostic biomarkers will represent an important step toward treatment. Once patients with preclinical AD [95] can be accurately identified, clinical treatments will have a better chance at slowing or stopping the disease progression.

While the results presented here show white matter decline, clinical use of DTI in AD diagnosis will likely be more valuable in combination with information from other biomarkers. It seems unlikely that a single prognostic biomarker will ever be discovered and that the best hope for early detection of AD lies in the form of a combination of modalities [96]. For example, a prognostic risk could be calculated from a combination of amyloid imaging, hippocampal volume, hippocampal connectivity, and CSF measurements, combined with genetic risk factors. These measurements in combination could give a risk likelihood score, which might allow for potential treatment options to be considered [96].

This multi-modal biomarker theory is the basis for the ADNI database [97]. ADNI is designed to collect a wide range of information at regular time points in a large patient population (a large scale, longitudinal, multi-modal study). Ideally, once the sample is large enough, researchers can take current AD subjects and look retrospectively at various imaging data to a time before cognitive symptoms existed. The results presented in this thesis provide a rationale for longitudinal assessment of WM abnormalities in individuals with MCI, such as comparison between the trajectories of MCI who progress to dementia and those who don't. This comparison would take excess noise out of the study that is being introduced by MCI patients that will never go on to develop AD. At writing, no ADNI or MCSA subjects with DTI baseline scans had converted to AD making this analysis a topic for future research.

As technology improves we continue to get better and more precise tools for measuring the brain. Larger magnets and better scanning parameters are just two of the more obvious developments allowing for better *in vivo* imaging sensitivity [98, 99]. Hopefully soon, MRI data obtained high field MRI (i.e. 7 Tesla) will greatly expand the results presented in this thesis. In essence improvement in imaging sensitivity

will lower the hypothetical 'detection threshold' depicted in the in figure 3.1 allowing for AD brain abnormalities to be detected in a preclinical stage. Higher sensitivity is a vital step in the quest to identify novel prognostic biomarkers.

Alzheimer's disease causes a devastating toll on the cognition of its patients and there is currently little effective treatment [2]. Despite these shortcomings there are reasons for hope. There are a number of large-scale databases, such ADNI, currently running that will allow large scale, longitudinal multimodal study of Alzheimer's disease. Utilization of the multimodal aspects of these databases has only just begun.

Increased awareness and research funding are already making there way to both the Canadian and US governments. The Canadian Institute of Health research recently awarded $49.5 million for the Canadian longitudinal study on aging to study 50,000 Canadians over the next 2 decades [100]. Additionally, the Obama administration announced a plan calling for a decade long study to comprehensively map brain activity [101]. In the press conference Alzheimer's disease was specifically mentioned as one of the areas that could benefit from the study. This is obviously incredibly ambitious but the fact that the study of the brain and in particular Alzheimer's disease is being made a political priority is a good sign for research funding and eventual breakthrough.

Bearing in mind all the limitations previously discussed, we were able to demonstrate white matter abnormalities in both AD and aMCI patient populations as compared to cognitively normal subjects. Continued study of DTI combined with other potential biomarkers could lead to a better understanding of the pathological progression of Alzheimer's disease and potentially effective treatment options.

Bibliography

1.   Morris JC. Clinical dementia rating: a reliable and valid diagnostic and staging measure for dementia of the Alzheimer type. International Psychogeriatrics 1997;9:173-176.
2.   Alzheimer's_Society. Rising Tide: The Impact of Dementia on Canadian Society, 2010.
3.   Gauthier S, Reisberg B, Zaudig M, et al. Mild cognitive impairment. The Lancet 2006;367:1262-1270.
4.   Petersen R, Aisen P, Beckett L, et al. Alzheimer's Disease Neuroimaging Initiative (ADNI): clinical characterization. Neurology 2010;74:201.
5.   Braak H, Braak E. Neuropathological stageing of Alzheimer-related changes. Acta Neuropathol 1991;82:239-259.
6.   Brun A, Englund E. A white matter disorder in dementia of the Alzheimer type: a pathoanatomical study. Annals of neurology 1986;19:253-262.
7.   Gomez-Isla T, Price JL, McKeel DW, Jr., Morris JC, Growdon JH, Hyman BT. Profound loss of layer II entorhinal cortex neurons occurs in very mild Alzheimer's disease. J Neurosci 1996;16:4491-4500.
8.   Morrison JH, Hof PR. Life and death of neurons in the aging brain. Science 1997;278:412.
9.   Schneider JA, Arvanitakis Z, Leurgans SE, Bennett DA. The neuropathology of probable Alzheimer disease and mild cognitive impairment. Ann Neurol 2009;66:200-208.
10.   Cummings JL, Doody R, Clark C. Disease-modifying therapies for Alzheimer disease: challenges to early intervention. Neurology 2007;69:1622-1634.
11.   Petersen R. Mild cognitive impairment as a diagnostic entity. Journal of Internal Medicine 2004;256:183-194.
12.   Rountree S, Waring S, Chan W, Lupo P, Darby E, Doody R. Importance of subtle amnestic and nonamnestic deficits in mild cognitive impairment: prognosis and conversion to dementia. Dementia and geriatric cognitive disorders 2007;24:476-482.
13.   Chen TF, Chen YF, Cheng TW, Hua MS, Liu HM, Chiu MJ. Executive dysfunction and periventricular diffusion tensor changes in amnesic mild cognitive impairment and early Alzheimer's disease. Human Brain Mapping 2009;30:3826-3836.
14.   Stokin GB, Goldstein LSB. Axonal transport and Alzheimer's disease. Annu Rev Biochem 2006;75:607-627.
15.   Wang DS, Bennett DA, Mufson EJ, Mattila P, Cochran E, Dickson DW. Contribution of changes in ubiquitin and myelin basic protein to age-related cognitive decline. Neuroscience research 2004;48:93-100.
16.   Bartzokis G, Cummings JL, Sultzer D, Henderson VW, Nuechterlein KH, Mintz J. White matter structural integrity in healthy aging adults and patients with Alzheimer disease: a magnetic resonance imaging study. Archives of neurology 2003;60:393.
17.   Lue LF, Rydel R, Brigham EF, et al. Inflammatory repertoire of Alzheimer's disease and nondemented elderly microglia in vitro. Glia 2001;35:72-79.
18.   Charlton R, Barrick T, McIntyre D, et al. White matter damage on diffusion tensor imaging correlates with age-related cognitive decline. Neurology 2006;66:217-222.

19.   Duan JH, Wang HQ, Xu J, et al. White matter damage of patients with Alzheimer‚Äôs disease correlated with the decreased cognitive function. Surgical and Radiologic Anatomy 2006;28:150-156.
20.   Albert M, Naeser MA, Levine HL, Garvey AJ. Ventricular size in patients with presenile dementia of the Alzheimer's type. Archives of neurology 1984;41:1258.
21.   Driscoll I, Davatzikos C, An Y, et al. Longitudinal pattern of regional brain volume change differentiates normal aging from MCI. Neurology 2009;72:1906-1913.
22.   Guttmann CRG, Jolesz FA, Kikinis R, et al. White matter changes with normal aging. Neurology 1998;50:972-978.
23.   Basser PJ, Mattiello J, LeBihan D. MR diffusion tensor spectroscopy and imaging. Biophys J 1994;66:259-267.
24.   Jbabdi S. Modeling Of DTI. In: FSL and FreeSurfer Course; 2009; San Francisco 2009.
25.   Agrawal A, Kapfhammer JP, Kress A, et al. Josef Klingler's Models of White Matter Tracts: Influences on Neuroanatomy, Neurosurgery, and Neuroimaging. Neurosurgery 2011;69:238.
26.   Ludwig E, Klingler J. Atlas cerebri humani: Der innere Aufbau des Gehirns, dargestellt auf Grund makroskopischer Präparate: la structure interne du cerveau demontrée sur les préparations macroscopiques: the inner structure of the brai demonstrated on the basis of macroscopical preparations: la aruitectura interna del cerebro demonstrada mediante preparaciones macroscópicas: Karger, 1956.
27.   Catani M. The rises and falls of disconnection syndromes. Brain 2005;128:2224.
28.   Staton RD, Brumback RA, Wilson H. Reduplicative paramnesia: A disconnection syndrome of memory. Cortex: A Journal Devoted to the Study of the Nervous System and Behavior 1982.
29.   Tucker DM, Roeltgen DP, Tully R, Hartmann J. Memory dysfunction following unilateral transection of the fornix: A hippocampal disconnection syndrome. Cortex: A Journal Devoted to the Study of the Nervous System and Behavior 1988.
30.   Fellgiebel A, Wille P, Muller MJ, et al. Ultrastructural hippocampal and white matter alterations in mild cognitive impairment: a diffusion tensor imaging study. Dement Geriatr Cogn Disord 2004;18:101-108.
31.   Muller MJ, Greverus D, Weibrich C, et al. Diagnostic utility of hippocampal size and mean diffusivity in amnestic MCI. Neurobiol Aging 2007;28:398-403.
32.   Rose SE, McMahon KL, Janke AL, et al. Diffusion indices on magnetic resonance imaging and neuropsychological performance in amnestic mild cognitive impairment. J Neurol Neurosurg Psychiatry 2006;77:1122-1128.
33.   Zhang Y, Schuff N, Jahng GH, et al. Diffusion tensor imaging of cingulum fibers in mild cognitive impairment and Alzheimer disease. Neurology 2007;68:13-19.
34.   Stebbins GT, Murphy CM. Diffusion tensor imaging in Alzheimer's disease and mild cognitive impairment. Behav Neurol 2009;21:39-49.
35.   Medina D, DeToledo-Morrell L, Urresta F, et al. White matter changes in mild cognitive impairment and AD: A diffusion tensor imaging study. Neurobiol Aging 2006;27:663-672.
36.   Bai F, Zhang Z, Watson DR, Yu H, Shi Y, Yuan Y. Abnormal white matter independent of hippocampal atrophy in amnestic type mild cognitive impairment. Neuroscience letters 2009;462:147-151.
37.   Chua TC, Wen W, Slavin MJ, Sachdev PS. Diffusion tensor imaging in mild cognitive impairment and Alzheimer's disease: a review. Curr Opin Neurol 2008;21:83-92.
38.   Agosta F, Pievani M, Sala S, et al. White matter damage in Alzheimer disease and its relationship to gray matter atrophy. Radiology 2011;258:853-863.

39.   Bosch B, Arenaza-Urquijo EM, Rami L, et al. Multiple DTI index analysis in normal aging, amnestic MCI and AD. Relationship with neuropsychological performance. Neurobiol Aging 2012;33:61-74.

40.   Douaud G, Jbabdi S, Behrens TE, et al. DTI measures in crossing-fibre areas: increased diffusion anisotropy reveals early white matter alteration in MCI and mild Alzheimer's disease. Neuroimage 2011;55:880-890.

41.   O'Dwyer L, Lamberton F, Bokde AL, et al. Multiple indices of diffusion identifies white matter damage in mild cognitive impairment and Alzheimer's disease. PloS one 2011;6:e21745.

42.   Basser PJ, Pajevic S, Pierpaoli C, Duda J, Aldroubi A. In vivo fiber tractography using DT-MRI data. Magn Reson Med 2000;44:625-632.

43.   Pievani M, Agosta F, Pagani E, et al. Assessment of white matter tract damage in mild cognitive impairment and Alzheimer's disease. Hum Brain Mapp 2010;31:1862-1875.

44.   Zhou Y, Dougherty JH, Jr., Hubner KF, Bai B, Cannon RL, Hutson RK. Abnormal connectivity in the posterior cingulate and hippocampus in early Alzheimer's disease and mild cognitive impairment. Alzheimers Dement 2008;4:265-270.

45.   Behrens TE, Berg HJ, Jbabdi S, Rushworth MF, Woolrich MW. Probabilistic diffusion tractography with multiple fibre orientations: What can we gain? Neuroimage 2007;34:144-155.

46.   Bozzali M, Parker GJ, Serra L, et al. Anatomical connectivity mapping: a new tool to assess brain disconnection in Alzheimer's disease. Neuroimage 2011;54:2045-2051.

47.   Campbell JSW, Savadjiev, P., Siddiqi, K. and Pike, G.B. . Validation and regularization in diffusion MRI tractography. IEEE International Symposium on Biomedical Imaging Conference Proceedings 2006:pages 351-354.

48.   Jiang H, van Zijl PC, Kim J, Pearlson GD, Mori S. DtiStudio: resource program for diffusion tensor computation and fiber bundle tracking. Comput Methods Programs Biomed 2006;81:106-116.

49.   Jack Jr CR, Knopman DS, Jagust WJ, et al. Hypothetical model of dynamic biomarkers of the Alzheimer's pathological cascade. Lancet neurology 2010;9:119.

50.   Mufson EJ, Binder L, Counts SE, et al. Mild cognitive impairment: pathology and mechanisms. Acta Neuropathol 2012;123:13-30.

51.   Clerx L, Visser PJ, Verhey F, Aalten P. New MRI Markers for Alzheimer's Disease: A Meta-Analysis of Diffusion Tensor Imaging and a Comparison with Medial Temporal Lobe Measurements. Journal of Alzheimer's Disease 2012;29:405-429.

52.   Sexton CE, Mackay CE, Ebmeier KP. A systematic review of diffusion tensor imaging studies in affective disorders. Biological psychiatry 2009.

53.   Gouw A, Seewann A, Vrenken H, et al. Heterogeneity of white matter hyperintensities in Alzheimer's disease: post-mortem quantitative MRI and neuropathology. Brain 2008;131:3286-3298.

54.   Behrens TE, Woolrich MW, Jenkinson M, et al. Characterization and propagation of uncertainty in diffusion-weighted MR imaging. Magn Reson Med 2003;50:1077-1088.

55.   Petersen RC, Parisi JE, Dickson DW, et al. Neuropathologic features of amnestic mild cognitive impairment. Arch Neurol 2006;63:665-672.

56.   Beattie BL. Consent in Alzheimer's disease research: risk/benefit factors. Can J Neurol Sci 2007;34 Suppl 1:S27-31.

57.   Schmidt M. Rey Auditory Verbal Learning Test: RAVLT: a Handbook: Western Psychological Services, 1996.

58.   Maes F, Collignon A, Vandermeulen D, Marchal G, Suetens P. Multimodality image registration by maximization of mutual information. IEEE Trans Med Imaging 1997;16:187-198.
59.   Berg L. Clinical dementia rating (CDR). Psychopharmacology bulletin 1988;24:637.
60.   Folstein MF, Folstein SE, McHugh PR. "Mini-mental state". A practical method for grading the cognitive state of patients for the clinician. J Psychiatr Res 1975;12:189-198.
61.   Aisen PS, Petersen RC, Donohue MC, et al. Clinical Core of the Alzheimer's Disease Neuroimaging Initiative: progress and plans. Alzheimer's & Dementia 2010;6:239-246.
62.   Wechsler D. WMS-R: Wechsler Memory Scale--Revised: manual: Psychological Corporation San Antonio, 1987.
63.   Lucas JA, Ivnik RJ, Smith GE, et al. Mayo's older Americans normative studies: category fluency norms. J Clin Exp Neuropsychol 1998;20:194-200.
64.   Tierney MC, Fisher RH, Lewis AJ, et al. The NINCDS-ADRDA Work Group criteria for the clinical diagnosis of probable Alzheimer's disease A clinicopathologic study of 57 cases. Neurology 1988;38:359-359.
65.   Eskildsen SF, Coupé P, Fonov V, et al. BEaST: Brain extraction based on nonlocal segmentation technique. Neuroimage 2012;59:2362-2373.
66.   Sled JG, Zijdenbos AP, Evans AC. A nonparametric method for automatic correction of intensity nonuniformity in MRI data. Medical Imaging, IEEE Transactions on 1998;17:87-97.
67.   Fonov V, Evans AC, Botteron K, Almli CR, McKinstry RC, Collins DL. Unbiased average age-appropriate atlases for pediatric studies. Neuroimage 2011;54:313.
68.   Zijdenbos A, Forghani R, Evans A. Automatic quantification of MS lesions in 3D MRI brain data sets: Validation of INSECT. In: Medical Image Computing and Computer-Assisted Intervention — MICCAI'98. Heidelberg: Springer Berlin 1998: 439-448.
69.   Collins DE, AC. ANIMAL: validation and applications of non-linear registration-based segmentation. International Journal and Pattern Recognition and Artificial Intelligence 1997;11:1271-1294.
70.   Jenkinson M, Pechaud M, Smith S. BET2: MR-based estimation of brain, skull and scalp surfaces. In: Eleventh annual meeting of the organization for human brain mapping; 2005, 2005.
71.   Jenkinson M, Pechaud M, Smith S. BET2: MR-based estimation of brain, skull and scalp surfaces. In; 2005, 2005: 12-16.
72.   Behrens TE, Johansen-Berg H, Woolrich MW, et al. Non-invasive mapping of connections between human thalamus and cortex using diffusion imaging. Nat Neurosci 2003;6:750-757.
73.   Smith SM, Jenkinson M, Johansen-Berg H, et al. Tract-based spatial statistics: voxelwise analysis of multi-subject diffusion data. Neuroimage 2006;31:1487-1505.
74.   Collins DL, Neelin P, Peters TM, Evans AC. Automatic 3D intersubject registration of MR volumetric data in standardized Talairach space. Journal of computer assisted tomography 1994;18:192.
75.   Nichols TE, Holmes AP. Nonparametric permutation tests for functional neuroimaging: a primer with examples. Human Brain Mapping 2001;15:1-25.
76.   Miller A, Alston R, Corsellis J. Variation with age in the volumes of grey and white matter in the cerebral hemispheres of man: measurements with an image analyser. Neuropathology and applied neurobiology 2008;6:119-132.

77.   Vollmar C, O'Muircheartaigh J, Barker GJ, et al. Identical, but not the same: intra-site and inter-site reproducibility of fractional anisotropy measures on two 3.0T scanners. Neuroimage 2010;51:1384-1394.
78.   Zhuang L, Wen W, Zhu W, et al. White matter integrity in mild cognitive impairment: a tract-based spatial statistics study. Neuroimage 2010;53:16-25.
79.   Salat DH, Tuch DS, van der Kouwe AJ, et al. White matter pathology isolates the hippocampal formation in Alzheimer's disease. Neurobiol Aging 2010;31:244-256.
80.   Krstic D, Knuesel I. Deciphering the mechanism underlying late-onset Alzheimer disease. Nature reviews Neurology 2012.
81.   Cagnin A, Kassiou M, Meikle SR, Banati RB. In vivo evidence for microglial activation in neuro degenerative dementia. In: Acta Neurologica Scandinavica, 2006: 107-114.
82.   Okello A, Edison P, Archer HA, et al. Microglial activation and amyloid deposition in mild cognitive impairment: a PET study. Neurology 2009;72:56-62.
83.   Carter SF, Schöll M, Almkvist O, et al. Evidence for astrocytosis in prodromal Alzheimer disease provided by 11C-deuterium-L-deprenyl: a multitracer PET paradigm combining 11C-Pittsburgh compound B and 18F-FDG. Journal of Nuclear Medicine 2012;53:37-46.
84.   Nestor SM, Rupsingh R, Borrie M, et al. Ventricular enlargement as a possible measure of Alzheimer's disease progression validated using the Alzheimer's disease neuroimaging initiative database. Brain 2008;131:2443-2454.
85.   Duvernoy HM. The human hippocampus: functional anatomy, vascularization and serial sections with MRI: Springer, 2005.
86.   Wang K, Liang M, Wang L, et al. Altered functional connectivity in early Alzheimer's disease: A resting-state fMRI study. Human Brain Mapping 2006;28:967-978.
87.   Wang L, Zang Y, He Y, et al. Changes in hippocampal connectivity in the early stages of Alzheimer's disease: evidence from resting state fMRI. Neuroimage 2006;31:496-504.
88.   Herholz K, Salmon E, Perani D, et al. Discrimination between Alzheimer dementia and controls by automated analysis of multicenter FDG PET. Neuroimage 2002;17:302-316.
89.   Delbeuck X, Van der Linden M, Collette F. Alzheimer'Disease as a Disconnection Syndrome? Neuropsychology review 2003;13:79-92.
90.   Giorgio A, Watkins K, Chadwick M, et al. Longitudinal changes in grey and white matter during adolescence. Neuroimage 2010;49:94-103.
91.   Roosendaal S, Geurts J, Vrenken H, et al. Regional DTI differences in multiple sclerosis patients. Neuroimage 2009;44:1397-1403.
92.   Jack Jr CR, Knopman DS, Jagust WJ, et al. Tracking pathophysiological processes in Alzheimer's disease: an updated hypothetical model of dynamic biomarkers. The Lancet Neurology 2013;12:207-216.
93.   Georganopoulou DG, Chang L, Nam J-M, et al. Nanoparticle-based detection in cerebral spinal fluid of a soluble pathogenic biomarker for Alzheimer's disease. Proceedings of the National Academy of Sciences of the United States of America 2005;102:2273-2276.
94.   Jack CR, Lowe VJ, Weigand SD, et al. Serial PIB and MRI in normal, mild cognitive impairment and Alzheimer's disease: implications for sequence of pathological events in Alzheimer's disease. Brain 2009;132:1355-1365.
95.   Sperling RA, Aisen PS, Beckett LA, et al. Toward defining the preclinical stages of Alzheimer's disease: Recommendations from the National Institute on Aging-Alzheimer's Association workgroups on diagnostic guidelines for Alzheimer's disease. Alzheimer's and Dementia 2011;7:280-292.

96.   Perrin RJ, Fagan AM, Holtzman DM. Multimodal techniques for diagnosis and prognosis of Alzheimer's disease. Nature 2009;461:916-922.
97.   Mueller SG, Weiner MW, Thal LJ, et al. Ways toward an early diagnosis in Alzheimer's disease: The Alzheimer's Disease Neuroimaging Initiative (ADNI). Alzheimer's and Dementia 2005;1:55-66.
98.   Kerchner GA, Deutsch GK, Zeineh M, Dougherty RF, Saranathan M, Rutt BK. Hippocampal CA1 apical neuropil atrophy and memory performance in Alzheimer's disease. Neuroimage 2012.
99.   Li X, Vikram DS, Lim IAL, Jones CK, Farrell JA, van Zijl P. Mapping Magnetic Susceptibility Anisotropies of White Matter< i> in vivo</i> in the Human Brain at 7 Tesla. Neuroimage 2012.
100.   Teotonio I. Landmark study on aging to follow 50,000 Canadians over the next two decades. Toronto Star 2012 Apr 24 2012.
101.   MARKOFF J. Obama Seeking to Boost Study of Human Brain. The New York Times 2013.
102.   Collins DL, Neelin P, Peters TM, Evans AC. Automatic 3D intersubject registration of MR volumetric data in standardized Talairach space. Journal of computer assisted tomography 1994;18:192-205.
103.   Englund E, Sjobeck M, Brockstedt S, Latt J, Larsson EM. Diffusion tensor MRI post mortem demonstrated cerebral white matter pathology. J Neurol 2004;251:350-352.
104.   Basser PJ, Pierpaoli C. Microstructural and physiological features of tissues elucidated by quantitative-diffusion-tensor MRI. Journal of Magnetic Resonance-Series B 1996;111:209-219.
105.   Woolrich MW, Jbabdi S, Patenaude B, et al. Bayesian analysis of neuroimaging data in FSL. Neuroimage 2009;45:S173-186.

Appendix 1: Extended Method Explanation

T1 Pipeline

Using an in-house processing pipeline, the T1 MRI underwent the following processes:

(1) The T1 MRI is skull stripped meaning a mask was created that excluded non-brain tissue [65]. This mask is primarily used for registration purposes.

(2) The t1 MRI is corrected for non-uniformities (NU correct) [66]. The purpose of this stage is to correct for signal in homogeneity usually due to a non-uniform RF (Radio Frequency) field. A simplified way to see it is before the correction grey matter in the fontal lobe will have different values than grey matter in the occipital lobes. The NU correct makes it so the grey matter through out the brain has approximately the same value.

(3) The T1-weighted image is registered to the MNI-151 space [102] using mutual information with a linear transformation with 9 free parameters. Subsequently a nonlinear transformation is applied in order to warp the t1 image to the best possible fit. In order to minimize anatomical variability, a 4mm isotropic Jacobean field is used. This nonlinear transformation (from diffusion native space to MNI space) was then inverted in order to allow images to be moved from MNI space to diffusion native space nonlinearly.

(4) The T1 is then classified into grey matter, white matter, and cerebrospinal fluid using INSECT, an automated classification algorithm [68].

(5) The classified image was automatically labeled using Automatic, Nonlinear, Imaging Matching and Anatomical Labeling (ANIMAL)[69]. ANIMAL uses an anatomical template to generate an unbiased probabilistic parcellation of each structural MRI.

Figure 3.1: Visual Depiction of the T1 MRI Pipeline

Structural MRI   Skull Strip   Nu Correct   Registration (nonlinear)   Classify   Segment
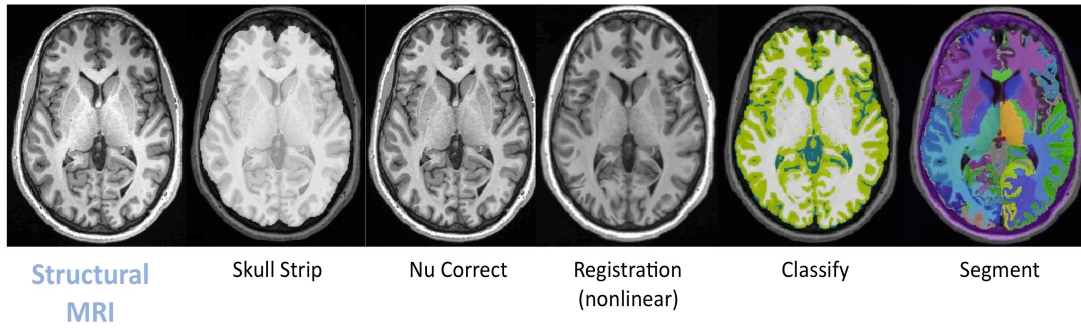
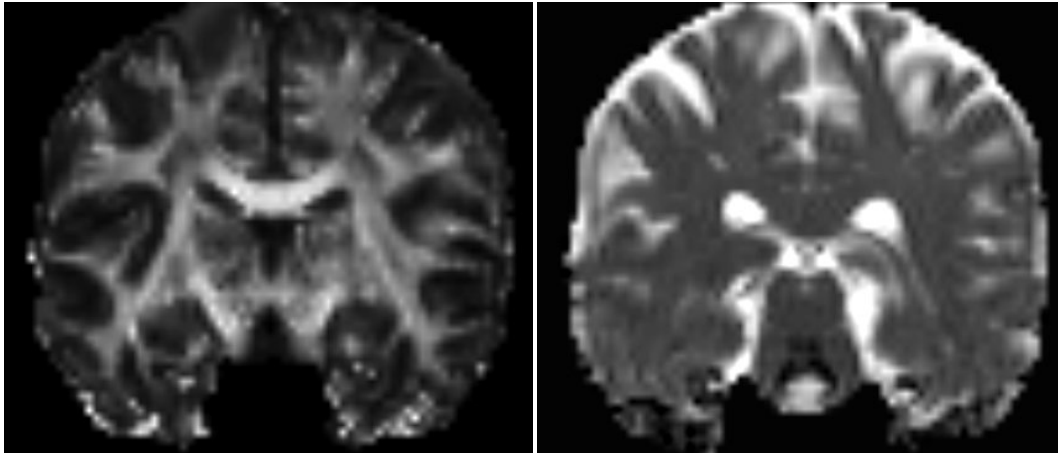**Fractional Anisotropy and Mean Diffusivity**

Fractional anisotropy (FA) is a unitless number between 0 and 1 used to describe the white matter structural organization by modeling the restriction of water diffusivity using DTI data. A value of 0 signifies the water is completely unconstrained and can move freely in any direction (a water molecule in the middle of a lake). A value of 1 signifies the water is perfectly constrained meaning it can only move one of two directions (forward or back). Equation 1 is used to determine the FA value of a given voxel.

$$\text{Fractional Anisotropy (FA)} = \frac{\sqrt{(\lambda 1 - \lambda 2)^2 + (\lambda 2 - \lambda 3)^2 + (\lambda 1 - \lambda 3)^2}}{\sqrt{2}\sqrt{\lambda 1^2 + \lambda 2^2 + \lambda 3^2}} \quad (1)$$

On a group level, reduction of FA indicates tissue disorganization and loss of connections. Using post mortem histological studies, it has been shown that the degree of white matter pathology correlated significantly with gradually lower FA values [103]. Mean diffusivity (MD) expresses the free water diffusion in a voxel. It is generally measured in millimeters squared per second (mm^2/s). Equation 2 is used to determine the MD of a given voxel.

$$\text{Mean Diffusivity (MD)} = \frac{\lambda 1 + \lambda 2 + \lambda 3}{3} \quad (2)$$

FA and MD were both first proposed in 1996 by Basser and Pierpaoli [104].

Figure 3.2: Example of FA and MD images

A: Example of Fractional Anisotropy **B**: Example of Mean Diffusivity

Fiber Tracking

First a seed region of interest (ROI) is automatically generated on the individual T1 using ANIMAL [69]. In this case the seed regions are drawn in both the left and right hippocampus. These ROIs are then nonlinear resampled to each participant's native diffusion space. An inspection is preformed to ensure accurate placement. The ROIs are to be used as seed regions for the probabilistic fiber tracking.

The probabilistic fiber tracking is done using an in-house pipeline based on FMRIB's Diffusion Toolbox (FSL), part of the FMRIB Software Library tool [105]. Hippocampal probabilistic fiber- maps were generated from the diffusion-weighed image for each subject using the following process:

Step 1: Preprocessing. Non-brain tissue is removed from diffusion-weighted images using BET2 [70] and are motion corrected using eddy-correct.

Step 2: Fiber direction. At each voxel in the diffusion image, a probability distribution of fiber direction is generated using FSL-BedpostX [72]. To account for non-dominant tracks and crossing fibers, a maximum of 2 fiber directions were modeled per voxel. This has been shown to significantly improve fiber tracking results [45].

Step 3: Probabilistic connectivity from a seed voxel. At a given voxel, 5000 sample fibers are sent out using FSL-probtrackx. For each fiber sample, a sample

direction is drawn from the probabilistic map generated in the previous step. The sample fiber proceeds at a fixed distance of 0.5mm in this direction, then samples another fiber direction from the current voxel's fiber direction map and moves again. This process is repeated, where a fiber samples a direction, moves 0.5mm to a new position and then samples a new direction again, until a the fiber reaches the edge of the brain or the fiber loops back on itself. Thus a probabilistic tractography map is generated for a given seed voxel such that each voxel in the brain has a number between 0 and 5000 representing the total number of sample fibers from the seed voxel that passed through that voxel of the brain. A probability of connection can be determined where the number of sample fibers that reach target voxel t divided by the number samples sent out from seed voxel s is probability p. That is to say, p represents the probability that the major fiber track passing through voxel s also passes through voxel t [54].

Step 4: Regional tractography. Variation of brain structure between individuals makes seed point selection difficult. As such it makes sense from both a practical and theoretical perspective to use anatomical structures as seed regions rather than a single seed voxel. To accomplish this a regional tractography method was developed. This process is repeated for each ROI for each subject. For a given seed region a probabilistic fiber map is created for each voxel in the region as defined in step 3. Thus n probabilistic fiber tracking maps were generated where n is the number of voxels in the seed region. These maps are combined to make one probabilistic fiber-tracking map for the entire seed region. To do this, all voxel-based fiber-tracking maps were aligned. The probability at each voxel in the new regional connectivity map was computed as the maximum value of any of the n fiber tracking maps at that voxel. Thus each voxel in this new regional tractography map still had a number between 0 and 5000. The value in a given voxel, divided by 5000, now represented the probability of that voxel being connected to the seed region.